ORGANOMETALLICS
Article

Organometallics **2010,** *29,* 3753–3764 3753
DOI: 10.1021/om100465d

Structure and Reactivity of Neutral and Cationic *trans*-*N*,*N*′-Dibenzylcyclam Zirconium Alkyl Complexes

Rui F. Munhá,[†,‡] M. Augusta Antunes,[†] Luis G. Alves,[†] Luis F. Veiros,[†] Michael D. Fryzuk,[‡] and Ana M. Martins*[,†]

[†]*Centro de Química Estrutural, Instituto Superior Técnico, Avenida Rovisco Pais, No. 1, 1049-001 Lisboa, Portugal, and* [‡]*Department of Chemistry, The University of British Columbia, 2036 Main Mall, Vancouver, British Columbia, Canada, V6T 1Z1*

Received May 14, 2010

Reactions of (Bn_2Cyclam)$ZrCl_2$ (**1**) (where Bn_2Cyclam = *trans*-N,N′$(PhCH_2)_2$Cyclam) with appropriate alkylating reagents produced (Bn_2Cyclam)ZrR_2 (R = Me (**2**), CH_2Ph (**3**), ^{n}Bu (**4**), CCPh (**5**)). Activation of the *ortho* C−H bond of the two macrocycle benzyl substituents in complexes **2**, **3**, and **4** was thermally induced, leading to the formation of a bis(*ortho*-metalated) complex, $((C_6H_4CH_2)_2$Cyclam)Zr (**6**). This reaction proceeds along with RH elimination and converts the original dianionic tetracoordinated cyclam in a tetraanionic hexacoordinated ligand where two new $Zr-C_{Ph}$ bonds complete the metal sphere. Treatment of **6** with one equivalent of HC≡CPh led to $((C_6H_4CH_2)$BnCyclam)Zr(CCPh) (**7**) via protonation of one $Zr-C_{Ph}$ bond by phenylacethylene. Further reaction of **7** with an excess of HC≡CPh led to **5**. The reactions of **2** and **3** with $B(C_6F_5)_3$ are strongly solvent dependent. Solvent-stabilized cationic species of formula [(Bn_2Cyclam)ZrR(Solv)]-[$RB(C_6F_5)_3$] were obtained from reactions of **2** in CD_2Cl_2 (**10**) or d_8-THF (**12**) and from **3** in d_8-THF (**9**). The reactions of **3** in CD_2Cl_2 or d_8-toluene gave [(Bn_2Cyclam)Zr(η^2-CH_2Ph)][$PhCH_2B(C_6F_5)_3$] (**8**). Finally, the reaction of **2** in d_8-toluene led to [(Bn_2Cyclam)Zr$(C_6F_5)\{CH_2B(C_6F_5)_2\}$] (**14**); the precursor of the latter is the zwitterionic [(Bn_2Cyclam)Zr$(CH_3)\{CH_3B(C_6F_5)_3\}$] (**11**), which then undergoes methane elimination and C_6F_5 migration from boron to zirconium. The mechanism of this reaction was studied by DFT and revealed that (i) methane elimination is assisted by one alpha-agostic C−H bond and (ii) migration of the C_6F_5 ring is supported by one bridging fluorine bond between the zirconium and one of the C_6F_5 rings that remains bonded to boron.

Introduction

Studies on the reactivity and stability of group 4 metal−alkyl species have had a tremendous impact on the discovery, understanding, and improvement of olefin polymerization catalysts.[1] It is now of general knowledge that generating active olefin polymerization catalysts requires an acidic metal species, where a metal−carbon bond and a vacant site occupy adjacent positions in the metal coordination sphere.[2] In addition, the ancillary ligands modulate the reactivity of the cationic metal−alkyl species by providing the correct balance of electronic and steric properties to the metal. However, the inability to predict the reactivity of a metal complex based on the choice of an ancillary ligand has made the search for new combinations of donor atoms and ligand frameworks a perennial research topic in coordination chemistry.[3]

Following our own efforts in the study of group 4 metal complexes supported by nitrogen-based ancillary ligands,[4] some of us have recently reported on the preparation of *trans*-disubstituted cyclam-based ligand precursors and their coordination chemistry to zirconium.[5] The saturated backbone

*To whom correspondence should be addressed. E-mail: ana.martins@ist.utl.pt.

(1) (a) Jordan, R. F. *Adv. Organomet. Chem.* **1991**, *32*, 325–387. (b) Bochmann, M. *J. Organomet. Chem.* **2004**, *689*, 3982–3998. (c) Chen, E. Y.-X.; Marks, T. *J. Chem. Rev.* **2000**, *100*, 1391–1434. (d) Deck, P. A.; Beswick, C. L.; Marks, T. J. *J. Am. Chem. Soc.* **1998**, *120*, 1772–1784. (e) Brintzinger, H. H.; Fischer, D.; Muelhaupt, R.; Rieger, B.; Waymouth, R. M. *Angew. Chem., Int. Ed. Engl.* **1995**, *34*, 1143–1170.

(2) (a) Klamo, S. B.; Wendt, O. F.; Henling, L. M.; Day, M. W.; Bercaw, J. E. *Organometallics* **2007**, *26*, 3018–3030. (b) Britovsek, G. J. P.; Gibson, V. C.; Wass, D. F. *Angew. Chem., Int. Ed.* **1999**, *38*, 428–447. (c) Beswick, C. L.; Marks, T. J. *Organometallics* **1999**, *18*, 2410–2412.

(3) (a) Agapie, T.; Henling, L. M.; DiPasquale, A. G.; Rheingold, A. L.; Bercaw, J. E. *Organometallics* **2008**, *27*, 6245–6256. (b) Gibson, V. C.; Spitzmesser, S. K. *Chem. Rev.* **2003**, *103*, 283–315. (c) Coates, G. W.; Hustad, P. D.; Reinartz, S. *Angew. Chem., Int. Ed.* **2002**, *41*, 2236–2257. (d) Shah, S. A. A.; Dorn, H.; Voigt, A.; Roesky, H. W.; Parisini, E.; Schmidt, H.-G.; Noltemeyer, M. *Organometallics* **1996**, *15*, 3176–3181.

(4) (a) Ferreira, M. J.; Matos, I.; Ascenso, J. R.; Duarte, M. T.; Marques, M. M.; Wilson, C.; Martins, A. M. *Organometallics* **2007**, *26*, 119–127. (b) Ferreira, H.; Dias, A. R.; Duarte, M. T.; Ascenso, J. R.; Martins, A. M. *Inorg. Chem.* **2007**, *46*, 750–755. (c) Ferreira, M. J.; Matos, I.; Ascenso, J. R.; Duarte, M. T.; Marques, M. M.; Wilson, C.; Martins, A. M. *Organometallics* **2006**, *26*, 119–127. (d) Barroso, S.; Cui, J.; Dias, A. R.; Duarte, M. T.; Ferreira, H.; Henriques, R. T.; Conceição Oliveira, M.; Ascenso, J. R.; Martins, A. M. *Inorg. Chem.* **2006**, *45*, 3532–3537. (e) Martins, A. M.; Ascenso, J. R.; Costa, S. M. B.; Dias, A. R.; Ferreira, H.; Ferreira, J. A. B. *Inorg. Chem.* **2005**, *44*, 9017–9022.

(5) (a) Munhá, R. F.; Alves, L. G.; Maulide, N.; Teresa Duarte, M.; Marko, I. E.; Fryzuk, M. D.; Martins, A. M. *Inorg. Chem. Commun.* **2008**, *11*, 1174–1176. (b) Munhá, R. F.; Namorado, S.; Barroso, S.; Teresa Duarte, M.; Ascenso, J. R.; Dias, A. R.; Martins, A. M. *J. Organomet. Chem.* **2006**, *691*, 3853–3861.

Published on Web 08/13/2010

Scheme 1[a]

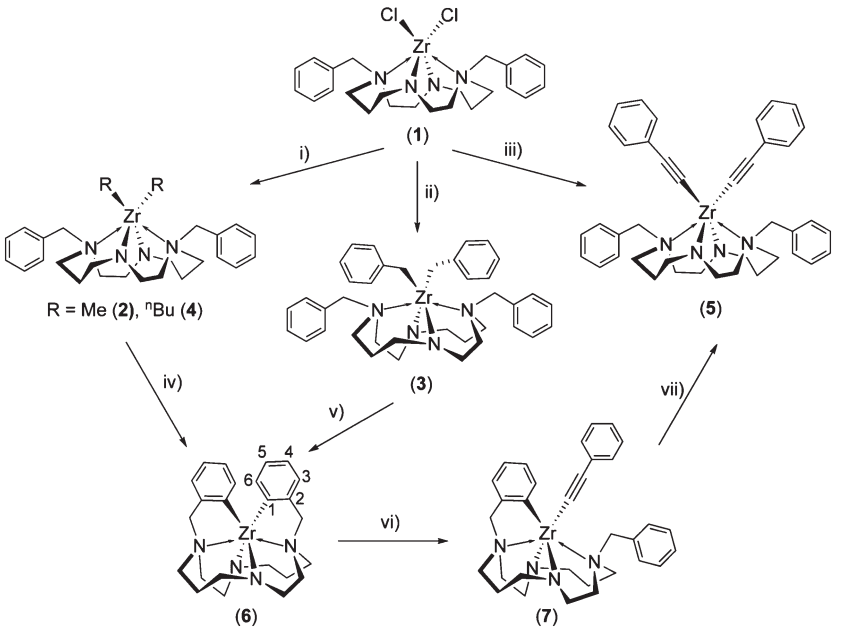

[a] Reaction conditions: (i) 2 MgClMe or 2 LiBu^n in THF; (ii) 2 MgClCH$_2$Ph in THF; (iii) 2 LiCCPh in THF; (iv) 70 °C, benzene, 2 h; (v) reflux, toluene, 72 h; (vi) HCCPh; (vii) HCCPh.

of the macrocyclic ligand confers an enhanced flexibility when compared to its unsaturated congeners, such as porphyrins or tetraazaannulenes.[6] Experimental and theoretical studies on amido, hydrazido, and imido complexes proved that different ancillary ligand conformations and metal coordination geometries are attained depending on the steric properties of the ligands present in the remaining coordination positions.[6]

Our interest in further exploring the reactivity of the zirconium systems led us to prepare the corresponding alkyl complexes and perform stoichiometric reactivity studies that are relevant to assess the potential of *trans*-disubstituted cyclam zirconium complexes as olefin polymerization catalysts.

Results and Discussion

Synthesis and Characterization of Zirconium Alkyl Complexes. The zirconium dichloride (Bn$_2$Cyclam)ZrCl$_2$ (**1**) can be prepared by a salt metathesis reaction between Li$_2$(Bn$_2$-Cyclam)(THF)$_2$ and ZrCl$_4$(THF)$_2$ or via a protonolysis reaction of the neutral ligand precursor with ZrCl$_2$(CH$_2$SiMe$_3$)$_2$(Et$_2$O)$_2$.[5] (Bn$_2$Cyclam)ZrCl$_2$ proved a convenient starting material for the synthesis of a variety of zirconium derivatives, and as shown in Scheme 1, complexes of general formula (Bn$_2$Cyclam)-ZrR$_2$ (R = Me (**2**), CH$_2$Ph (**3**), ^{n}Bu (**4**), CCPh (**5**)) are readily obtained by chloride metathesis using Mg or Li compounds as alkylating agents. Reaction of THF suspensions of (Bn$_2$-Cyclam)ZrCl$_2$ (**1**) with two equivalents of MgClR (R = CH$_3$, CH$_2$Ph) gave the corresponding zirconium dialkyl complexes (Bn$_2$Cyclam)ZrMe$_2$ (**2**) and (Bn$_2$Cyclam)Zr(CH$_2$Ph)$_2$ (**3**). **2** was isolated as an off-white solid in 63% yield upon extraction in toluene; it has a low solubility in aromatic solvents, and it is not stable at room temperature in solution, as attested by the ^{1}H NMR spectrum, where a singlet assigned to methane is identified at 0.16 ppm, which then increases over time. Its thermal instability constrains its preparation to small-scale reactions and hampers its isolation in high yield. The choice of alkylating agent also appears critical, as the use of a LiMe solution produces a complex mixture of compounds where only free H$_2$(Bn$_2$Cyclam) could be identified.

Under similar reaction conditions, **3** was prepared in 80% yield using the appropriate Grignard reagent (MgClCH$_2$Ph). The rapid conversion of the bright yellow THF suspension of (Bn$_2$Cyclam)ZrCl$_2$ into an intensely yellow-colored solution is indicative that the reaction proceeds faster than in the case of **2**; the higher solubility of the resulting complex **3** and the fact that it is more stable in solution prove to be important for further reactivity studies.

Reaction of **1** with two equivalents of Li^{n}Bu gives (Bn$_2$-Cyclam)Zr(^{n}Bu)$_2$ (**4**) in 86% yield. The formation of bis(alkyl) complexes containing β-hydrogens is unusual as they normally tend to undergo β-elimination reactions to give other products.[7] However, in what is becoming a trend in zirconium complexes supported by amido ligands, alkyl complexes of this type display an unexpected stability.[8]

(Bn$_2$Cyclam)Zr(CCPh)$_2$ (**5**) was synthesized on a preparative scale via salt metathesis; to a cold THF suspension of **1**, two equivalents of LiCCPh was added and **5** was isolated in 52% yield. This reaction is a convenient alternative synthetic route for the recently reported preparation of **5** via reaction of (Bn$_2$Cyclam)Zr(N$^{2,6\text{-}i\text{Pr}}$Ph) with an excess of phenylacetylene.[6]

The synthesis of mixed alkyl-chloride complexes by reaction of (Bn$_2$Cyclam)ZrCl$_2$ with one equivalent of each of the above-mentioned alkylating agents was attempted, but it was not possible to isolate the desired monosubstituted complexes.

(6) Munhá, R. F.; Veiros, L. F.; Duarte, M. T.; Fryzuk, M. D.; Martins, A. M. *Dalton Trans.* **2009**, 7494–7508.

(7) (a) Harney, M. B.; Keaton, R. J.; Fettinger, J. C.; Sita, L. R. *J. Am. Chem. Soc.* **2006**, *128*, 3420–3432. (b) Wendt, O. F.; Bercaw, J. E. *Organometallics* **2001**, *20*, 3891–3895.

(8) (a) Warren, T. H.; Schrock, R. R.; Davis, W. M. *Organometallics* **1998**, *17*, 308–321. (b) Schattenmann, F. J.; Schrock, R. R.; Davis, W. M. *Organometallics* **1998**, *17*, 989–992.

Once the alkyl-chloride complex is formed, the second substitution is apparently favored, generating a mixture of mono- and bis(alkyl) complexes that could not be separated.

The NMR spectra of compounds **2**−**5** display an average C_2 symmetry in solution, similar to the dichloride precursor. Thus, in the room-temperature ^{1}H NMR spectra 10 resonances can be identified, integrating to two protons each, assigned to the H_{anti} and H_{syn} methylenic protons of the macrocyclic ligand backbone. Given the complexity of the NMR spectra and the overlap of these resonances, the signals assigned to the benzylic protons of the ancillary ligand are generally diagnostic due to the fact that they are shifted to low field and show as a characteristic AB pattern ($^2J_{HH}$ = 14 Hz). The $^{13}C\{^1H\}$ NMR spectra confirm the average C_2 symmetry in solution of the metal complexes, as six resonances attributed to the ancillary ligand methylenic carbons and one set of aromatic signals are observed. Two-dimensional NMR experiments, such as COSY, NOESY, HMBC, and HSQC, were conducted in order to assign all proton and carbon resonances of the ancillary ligand set.

In the C_6D_6 ^{1}H NMR spectrum of (Bn$_2$Cyclam)ZrMe$_2$ (**2**), the AB pattern corresponding to the benzylic protons of the cyclam ligand is observed at 4.54 and 4.35 ppm, whereas the signal that accounts for the zirconium-bound methyl groups appears at 0.58 ppm as a singlet. The $^{13}C\{^1H\}$ NMR of **2** shows a distinct signal at 36.5 ppm that accounts for the two methyl groups. The ^{1}H NMR spectrum of (Bn$_2$Cyclam)Zr(CH$_2$Ph)$_2$ (**3**) shows two signals at 4.37 and 3.51 ppm that account for the diastereotopic benzylic protons of the ancillary ligand; another AB system, with each doublet integrating to two protons, is observed at 2.72 and 2.63 ppm ($^2J_{HH}$ = 9 Hz), corresponding to the methylenic protons of the benzyl groups bonded to zirconium. In the $^{13}C\{^1H\}$ NMR spectrum, the latter are characterized by one resonance at 66.1 ppm corresponding to the methylenic carbons and three distinguishable aromatic resonances at 150.6, 130.1, and 119.7 ppm, accounting for the *ipso*, *ortho*, and *para* carbons, respectively; the peak for the *meta* carbons is obscured by the deuterated solvent resonance. The chemical shifts of the methylenic and *ipso* carbons of the benzyl ligand are consistent with an η^1-coordination mode.[9] This was also confirmed by a gated-decoupled ^{13}C NMR experiment, where a $^1J_{CH}$ of 124 Hz for the methylenic carbon was observed.[10]

The C_6D_6 ^{1}H NMR spectrum of (Bn$_2$Cyclam)Zr(^{n}Bu)$_2$ (**4**) shows an AB pattern at 4.65 and 4.39 ppm that accounts for the benzylic protons of the ancillary ligand. The two *n*-butyl ligands are equivalent, as attested by the four signals identified in the $^{13}C\{^1H\}$ NMR spectrum. The methylene group bonded to zirconium has two inequivalent protons identified in the ^{1}H NMR spectrum at 1.05 and 0.60 ppm, whereas the remaining two methylene and methyl resonances are observed at 2.20, 1.81, and 1.25 ppm, respectively. The $^{13}C\{^1H\}$ NMR spectrum shows the broadening of one signal at 55.9 ppm, assigned to the [C3] chain of the macrocycle; this may hint at a fluxional process and was already observed in cyclam-based zirconium complexes, but low-temperature NMR experiments only led to further broadening of the peaks.

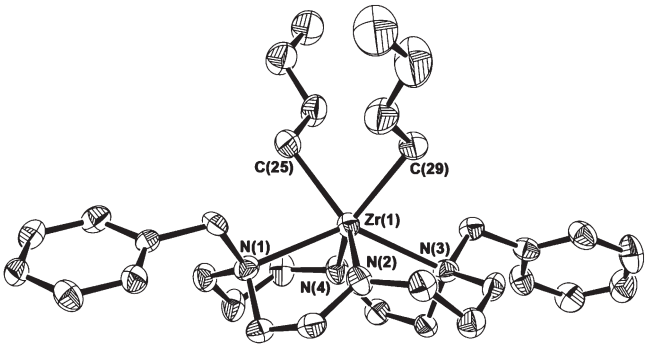

Figure 1. Solid-state molecular structure (ORTEP representation shown at 50% thermal ellipsoid probability) of (Bn$_2$Cyclam)Zr(^{n}Bu)$_2$ (**4**) as determined by X-ray crystallography. Selected bond lengths (Å) and angles (deg): Zr(1)−C(25) 2.340(5); Zr(1)−C(29) 2.318(5); Zr(1)−N(1) 2.456(4); Zr(1)−N(2) 2.099(4); Zr(1)−N(3) 2.474(4); Zr(1)−N(4) 2.093(4); C(25)−Zr(1)−C(29) 82.9(2); N(2)−Zr(1)−N(4) 117.33(18); N(1)−Zr(1)−N(3) 133.81(13); C(29)−Zr(1)−N(2) 93.57(18); C(29)−Zr(1)−N(4) 135.61(18); C(25)−Zr(1)−N(4) 93.55(19); C(25)−Zr(1)−N(2) 136.09(18).

The AB system corresponding to the benzylic protons of the macrocyclic ligand in (Bn$_2$Cyclam)Zr(CCPh)$_2$ (**5**) shows at 5.33 and 4.33 ppm. The phenylacetylenyl ligand is characterized by a distinguishable set of aromatic resonances at 7.65 and 7.10−7.00 ppm. In relation to the $^{13}C\{^1H\}$ NMR spectrum of the alkynyl ligand, besides one set of *ortho*, *meta*, and *para* carbons, three signals at 105.5, 127.0, and 149.9 ppm, corresponding to quaternary carbons, are observed. The resonances at 149.9 and 105.5 ppm are assigned to the triple-bonded carbon atoms, with the former corresponding to the zirconium-bonded carbon. The IR spectrum of **5** shows a characteristic band at 2069 cm^{-1}, attributed to the C≡C stretching vibration mode, which is significantly lower than that of free phenylacetylene ($\nu_{C\equiv C}$ = 2110 cm^{-1}).

Crystals of **4** were obtained from a cold diethyl ether solution. An ORTEP representation with selected bond lengths and angles is depicted in Figure 1. The macrocycle attains a conformation where the four nitrogens define an average plane with the metal center sitting 1.0280(22) Å above it. The bond distances of the macrocyclic nitrogen atoms to zirconium—2.093(4) and 2.099(4) Å for the Zr−N$_{amido}$ and 2.456(4) and 2.474(4) Å for the Zr−N$_{amine}$—are within the expected values[11] and compare to previously described complexes incorporating this macrocyclic ligand. The geometry around zirconium is best described as trigonal prismatic with the two *n*-butyl ligands *cis* to each other. The Zr−C bond lengths of 2.318(5) and 2.340(5) Å are within the expected values for alkyl ligands in Zr(IV) metal centers.[12] The C(25)−Zr−C(29) angle of 82.9(2)° is similar to the Cl(1)−Zr−Cl(2) angle of the dichloride precursor (84.76(3)°) and other related zirconium complexes, indicating that there is no steric hindrance caused by the *n*-butyl substituents.

Crystals of **3** suitable for X-ray diffraction were obtained from a concentrated toluene solution, and an ORTEP representation is depicted in Figure 2 with selected bond lengths

(9) (a) Kirillov, E.; Lavanant, L.; Thomas, C.; Roisnel, T.; Chi, Y.; Carpentier, J.-F. *Chem.—Eur. J.* **2007**, *13*, 923–935. (b) Chen, Y.-X.; Marks, T. J. *Organometallics* **1997**, *16*, 3649–3657.

(10) (a) Bochmann, M.; Lancaster, S. J. *Organometallics* **1993**, *12*, 633–640. (b) Jordan, R. F.; LaPointe, R. E.; Baenziger, N.; Hinch, G. D. *Organometallics* **1990**, *9*, 1539–1545. (c) Mintz, E. A.; Moloy, K. G.; Marks, T. J.; Day, V. W. *J. Am. Chem. Soc.* **1982**, *104*, 4692–4695.

(11) (a) Li, Y.; Turnas, A.; Ciszewski, J. T.; Odom, A. L. *Inorg. Chem.* **2002**, *41*, 6298–6306. (b) O'Connor, P. E.; Morrison, D. J.; Steeves, S.; Burrage, K.; Berg, D. J. *Organometallics* **2001**, *20*, 1153–1160.

(12) (a) Tonzetich, Z. J.; Lu, C. C.; Schrock, R. R.; Hock, A. S.; Bonitatebus, P. J., Jr. *Organometallics* **2004**, *23*, 4362–4372. (b) Mehrkhodavandi, P.; Schrock, R. R.; Bonitatebus, P. J., Jr. *Organometallics* **2002**, *21*, 5785–5798.

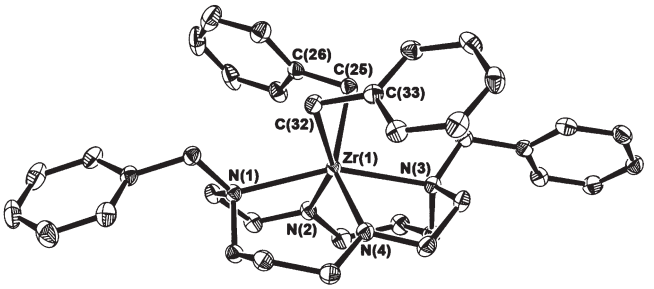

Figure 2. Solid-state molecular structure (ORTEP representation shown at 50% thermal ellipsoid probability) of $(Bn_2Cyclam)Zr(CH_2Ph)_2$ (**3**) as determined by X-ray crystallography. Selected bond lengths (Å) and angles (deg): Zr(1)−C(25) 2.3606(19); Zr(1)−C(32) 2.3902(17); Zr(1)−N(1) 2.4465(15); Zr(1)−N(2) 2.1144(15); Zr(1)−N(3) 2.4611(15); Zr(1)−N(4) 2.0951(16); C(25)−Zr(1)−C(32) 86.47(7); C(26)−C(25)−Zr(1) 106.90(12); C(33)−C(32)−Zr(1) 103.18(11); N(2)−Zr(1)−N(4) 106.23(6); N(1)−Zr(1)−N(3) 156.28(5); C(32)−Zr(1)−N(2) 151.29(6); C(32)−Zr(1)−N(4) 89.70(6); C(25)−Zr(1)−N(4) 148.93(6); C(25)−Zr(1)−N(2) 91.15(6).

and angles. The solid-state structure shows the expected *cis* coordination of the two benzyl ligands and the metal center perched on the macrocyclic cavity, as observed in all cyclam-based zirconium complexes reported to date. However, in **3** the geometry around the metal center is best described as distorted octahedral, with N(1), N(3), N(4), and C(25) occupying a slightly twisted square plane displaying a combined equatorial angle of 364.1° and N(2) and C(32) occupying the axial positions, with an N(2)−Zr−C(32) angle of 151.29(6)°. This result contrasts with previously described complexes incorporating this ligand set, as hitherto we have observed that the coordination geometries around the metal center vary between trigonal prismatic and tetrahedral.

An increase in the N(1)−Zr−N(3) angle from 133.81(13)° in **4** to 156.28(5)° in **3** is observed; this change is accompanied by a decrease in the N(2)−Zr−N(4) angle from 117.33(18)° in **4** to 106.23(6)° in **3**. Thus, in the case of **3** the macrocycle has such a conformational twist that it is not possible to define an average plane containing the four nitrogen donors. Interestingly, the C(25)−Zr−C(32) angle of 86.47(7)° shows that the new conformation of the ancillary ligand is not accompanied by a change of the relative positions of the two benzyl ligands, as this value compares to both **4** and the dichloride precursor. The $Zr-CH_2-C_{ipso}$ angles at 106.90(12)° and 103.18(11)° are in accordance with an η^1-coordination of the benzyl ligands, although the values are lower than expected for an sp^3-hybridized carbon, suggesting a weak $Zr-C_{ipso}$ interaction.[13] The $Zr-N_{amido}$ (2.0915(16) and 2.1144(15) Å) and the Zr−C bond lengths (2.3606(19) and 2.3902(17) Å) are within the observed values for other benzyl zirconium complexes.[14] Although the $Zr-N_{amine}$ bonds at 2.4465(15) and 2.4611(15) Å are somewhat elongated, they are comparable to previously reported hexacoordinated zirconium complexes incorporating this ligand.

Overall, the analysis of the solid-state molecular structures of **3** and **4** confirm what had been postulated before: the saturated ancillary ligand backbone allows for different conformations to be attained, depending on the ligands that occupy the remaining coordination positions.

Reactivity of the Zirconium Alkyl Complexes. The aforementioned instability of $(Bn_2Cyclam)ZrMe_2$ (**2**) in solution led us to investigate this reaction further. Heating a C_6D_6 solution of **2** at 70 °C over a two-hour period gave a new C_2-symmetric species for which the ^1H NMR spectrum does not show any resonance attributed to the zirconium-bound methyl groups and also displays a singlet at 0.16 ppm corresponding to dissolved methane. The 10 resonances, integrating to two protons each, assigned to the ligand backbone methylenic protons display a distinct pattern from starting complex **2**. In addition, the signals corresponding to the benzylic protons of the ligand appear at 4.81 and 3.60 ppm as an AB system (4.54 and 4.35 ppm in **2**). Integration of the aromatic region of the spectrum shows only eight protons, including a new resonance at 8.20 ppm that integrates to two protons. On the basis of the loss of methane and the observation of only eight aromatic protons, the new species was assigned as $((C_6H_4CH_2)_2$-Cyclam)Zr (**6**) (Scheme 1), resulting from C−H activation of the *ortho* protons of the benzyl groups of the ancillary ligand.[15] *Ortho*-metalation was confirmed by the $^{13}C\{^1H\}$ NMR spectrum; the signal attributed to the aromatic carbon bound to zirconium is observed at 188.5 ppm, and as expected, C(2) and C(6) are shifted to a lower field at 151.1 and 140.8 ppm, respectively (see Scheme 1 for labeling). In addition, six resonances corresponding to the methylenic carbons are observed between 63.3 and 26.4 ppm. Full NMR characterization of **6** was based on ^{13}C APT, HSQC, HMBC, and COSY experiments.

Under the same reaction conditions, $(Bn_2Cyclam)Zr(^nBu)_2$ (**4**) gives **6** and *n*-butane, which is identified in the ^1H NMR spectrum by two resonances at 1.25 and 0.85 ppm. Conversely, heating at 70 °C a C_6D_6 solution of $(Bn_2Cyclam)$-$Zr(CH_2Ph)_2$ (**3**) over a period of 12 h gives only a small amount of **6**; however, mild reflux of the benzene solution of **3** for 72 h resulted in complete conversion to **6**. The *ortho*-metalation reaction was not observed for $(Bn_2Cyclam)$-$Zr(CCPh)_2$ (**5**) upon reflux in C_6D_6. This result is consistent with the higher acidity of sp-hybridized carbons when compared to sp^3-carbon ligands.

The reaction of $(Bn_2Cyclam)ZrMe_2$ (**2**) with two equivalents of HC≡CPh was studied by NMR in C_6D_6 solution. At room temperature the reaction proceeds slowly with a yield of about 50% of **5** after 18 h. Heating the solution at 50 °C leads to the quantitative formation of **5** in 4 h. Under these reaction conditions, its formation may result from the direct reaction of **2** with HC≡CPh or, alternatively, from the reaction of **6**, formed *in situ* from the *ortho*-metalation reaction described above, with HC≡CPh. To evaluate whether this reaction may be considered an alternative path for the formation of **5**, the reaction of **6** with HC≡CPh in C_6D_6 was performed. The addition of one equivalent of HC≡CPh at room temperature led to the formation of **5** alongside a new species that was identified as **7** (Scheme 1) in a 1:2.5 ratio. The addition of a second equivalent of HC≡CPh to a solution containing **5**, **6**, and **7** results in the quantitative formation of **5** after heating at 50 °C for 4 h. The proton NMR spectrum of **7** reveals a C_1-symmetric species. The macrocyclic protons give rise to 20 resonances ranging from

(13) (a) Fryzuk, M. D.; Love, J. B.; Rettig, S. J. *Organometallics* **1998**, *17*, 846–853. (b) Giannini, L.; Solari, E.; De Angelis, S.; Ward, T. R.; Floriani, C.; Chiesi-Villa, A.; Rizzoli, C. *J. Am. Chem. Soc.* **1995**, *117*, 5801–5811.

(14) Kirillov, E.; Roisnel, T.; Razavi, A.; Carpentier, J.-F. *Organometallics* **2009**, *28*, 5036–5051.

(15) (a) Boehme, U.; Thiele, K. H. *Z. Anorg. Allg. Chem.* **1993**, *619*, 1488–1490. (b) Chmielewski, P. J.; Durlej, B.; Siczek, M.; Szterenberg, L. *Angew. Chem., Int. Ed.* **2009**, *48*, 8736–8739.

Scheme 2

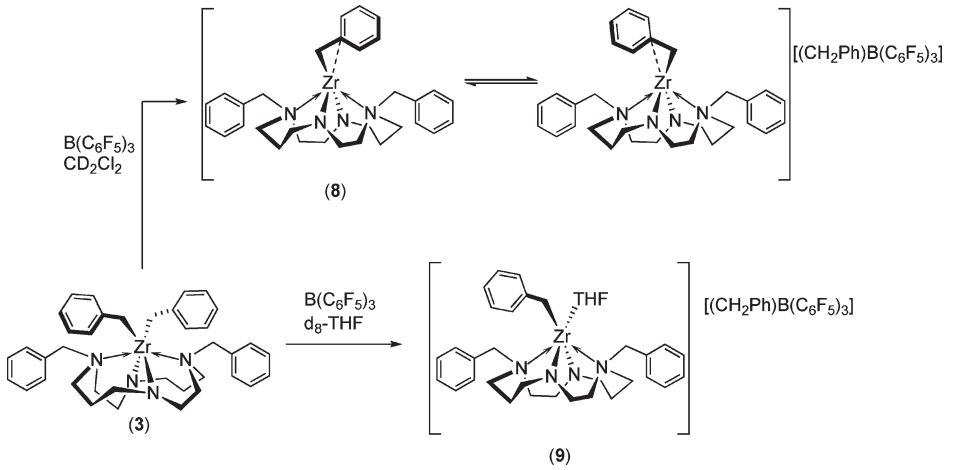

4.23 to 0.82 ppm. The methylenic protons of the macrocyclic benzyl substituents appear as two sets of AB systems, corresponding to a zirconium-bound benzyl group and to the non-*ortho*-metalated benzyl. The coordination of the aromatic ring to the metal is confirmed by a doublet at 8.97 ppm assigned to the new *ortho* proton and by the ^{13}C resonances at 188.3, 150.0, and 142.2 ppm, corresponding to C(1), C(2), and C(6), respectively (see Scheme 1 for labeling).

The reaction of $(Bn_2Cyclam)Zr(CH_2Ph)_2$ (**3**) with one equivalent of $B(C_6F_5)_3$ in d_2-dichloromethane affords a cationic species with a coordinated η^2-benzyl, $[(Bn_2Cyclam)Zr(\eta^2\text{-}CH_2Ph)][PhCH_2B(C_6F_5)_3]$ (**8**) (Scheme 2). The presence of a free tetrahedral boron anion is supported by a $\Delta(\delta F_{para} - \delta F_{meta})$ lower than 3 ppm (2.9 ppm) in the ^{19}F NMR spectrum and a single resonance at -12.9 ppm in the ^{11}B spectrum.[16] In the ^1H NMR spectrum, the signals corresponding to Zr-C*H*$_2$Ph appear as an AB system shifted downfield in comparison to its precursor (3.08 and 2.70 ppm in **8** vs 2.41 and 2.35 ppm in **3**), as reported for other cationic species.[17] The methylene protons bonded to boron give rise to one singlet at 2.86 ppm. The assignment of this resonance was confirmed by a $^{19}F-^1H$ HOESY experiment that showed a cross-peak with the *ortho*-F resonance of the C_6F_5 groups. The B-*C*H$_2$Ph carbon resonance was not observed in the ^{13}C spectrum but was identified through a $^1H-^{13}C$ HSQC experiment at 32.0 ppm. The identification of η^2-benzyl coordination in **8** is based on a gated-decoupled ^{13}C NMR spectrum, where an increase of the $^1J_{CH}$ of the resonance corresponding to the methylenic carbon from 124 Hz in **3** to 139 Hz is observed.[18] Moreover, the high-field shift observed for the *ipso* carbon of the benzyl group (139.4 ppm in **8** vs 150.8 ppm in **3**) suggests that the interaction between the zirconium and the aromatic ring is established through the C_{ipso} and not the aromatic C=C bond.[17b,c,19] The macrocycle proton and carbon NMR resonances are consistent with an average C_2 symmetry, suggesting an exchange processes between two possible conformations (Scheme 2). Low-temperature NMR studies did not slow the fluxional process, and only broadening of all proton resonances was observed.

The role of the solvent was investigated, and while carrying out the reaction on a noncoordinating solvent such as d_8-toluene produced the same outcome, the change to d_8-THF gives the solvent-stabilized cation $[(Bn_2Cyclam)Zr(CH_2Ph)(THF)][PhCH_2B(C_6F_5)_3]$ (**9**) (Scheme 2). The proton and carbon NMR spectra of **9** at room temperature are consistent with an average C_2-symmetry complex, implying a rapid exchange between coordinated and free solvent. The ^{11}B and ^{19}F NMR spectra confirm the formation of a cationic species; however in **9**, the zirconium-bound benzyl group is η^1-coordinated, as attested by the chemical shift of the *ipso* carbon at 147.1 ppm (similar to **3**) and a $^1J_{CH}$ of 125 Hz corresponding to the resonance of the methylenic carbon.

The reaction of one equivalent of $B(C_6F_5)_3$ with **2** was carried out at room temperature in CD_2Cl_2. The ^{19}F NMR spectrum reveals a set of signals with a $\Delta(\delta F_{para} - \delta F_{meta})$ of 2.7 ppm and a resonance at -14.9 ppm in the ^{11}B NMR spectrum, suggesting the formation of the cationic complex $[(Bn_2Cyclam)ZrMe(CD_2Cl_2)][B(C_6F_5)_3(CH_3)]$ (**10**) (Scheme 3).[16a] Abstraction of a methyl group from **2** by $B(C_6F_5)_3$ is also based on the observation of a singlet in the ^1H NMR spectrum at 0.49 ppm that shows a correlation to a carbon resonance at 11.0 ppm in the HSQC spectrum and is assigned to *C*H$_3$B. These data and a peak in the mass spectrum with m/z of 526.9 confirm the formation of $[B(C_6F_5)_3(CH_3)]^-$, supporting the formulation of **10**. The AB system due to the methylenic protons of the cyclam benzyl substituents is shifted to high field (4.03 and 3.77 ppm) in comparison to the parent complex (4.54 and 4.26 ppm). This effect is symptomatic of a cationic complex, as it is observed in all cations regardless of the solvent that stabilizes the metal center. Compound **10** is highly stable in CD_2Cl_2 solution, as the NMR spectra do not reveal any decomposition over several weeks at room temperature. The proton and carbon NMR spectra of **10** at room temperature are consistent with a metal complex with an average C_2 symmetry resulting from an exchange between free and coordinated solvent. On cooling the solution, broadening and overlapping of the resonances

(16) (a) Horton, A. D.; de With, J. *Chem. Commun.* **1996**, 1375–1376. (b) Shafir, A.; Arnold, J. *Organometallics* **2003**, *22*, 567–575. (c) Yang, X.; Stern, C. L.; Marks, T. J. *J. Am. Chem. Soc.* **1994**, *116*, 10015–10031. (d) Pellecchia, C.; Grassi, A.; Zambelli, A. *J. Mol. Catal.* **1993**, *82*, 57–65.

(17) (a) Amor, F.; Butt, A.; du Plooy, K. E.; Spaniol, T. P.; Okuda, J. *Organometallics* **1998**, *17*, 5836–5849. (b) Horton, A. D.; de With, J.; van der Linden, A. J.; van de Weg, H. *Organometallics* **1996**, *15*, 2672–2674. (c) Bochmann, M.; Lancaster, S. J.; Hursthouse, M. B.; Malik, K. M. A. *Organometallics* **1994**, *13*, 2235–2243.

(18) (a) Dryden, N. H.; Legzdins, P.; Phillips, E. C.; Trotter, J.; Yee, V. C. *Organometallics* **1990**, *9*, 882–884. (b) Lee, L.; Berg, D. J.; Bushnell, G. W. *Organometallics* **1997**, *16*, 2556–2561. (c) Jordan, R. F.; LaPointe, R. E.; Bajgur, C. S.; Echols, S. F.; Willett, R. *J. Am. Chem. Soc.* **1987**, *109*, 4111–4113.

(19) Scott, M. J.; Lippard, S. J. *Organometallics* **1998**, *17*, 1769–1773.

Scheme 3

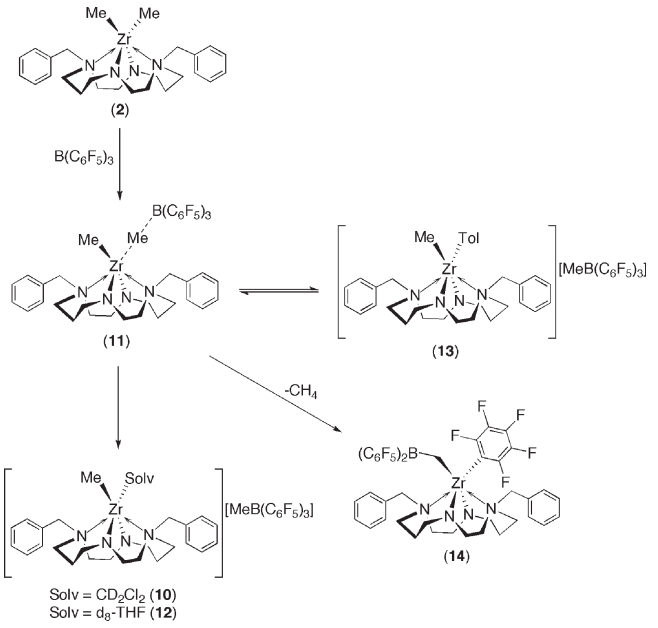

attributed to the macrocycle did not allow a limiting spectrum until −80 °C.

On the other hand, the reaction of $B(C_6F_5)_3$ with (Bn_2-Cyclam)$ZrMe_2$ (**2**) was carried out in a sealed NMR tube by addition of one equivalent of the borane to a frozen CD_2Cl_2 solution of the complex, and the reaction was followed by ^{19}F, ^{1}H, and ^{11}B NMR spectroscopy. At −80 °C the ^{1}H NMR spectrum is best described as a set of several broad resonances. Upon warming, these start to resolve, and at −20 °C the ^{19}F and ^{11}B NMR spectra indicate the formation of two species. The signals corresponding to the major product are consistent with a cationic species having the counterion $[B(C_6F_5)_3(CH_3)]^-$, as described for **10**. The minor product of this reaction is characterized by a signal at −4.2 ppm in the ^{11}B spectrum and a set of resonances in the ^{19}F spectrum with $\Delta(\delta F_{para} - \delta F_{meta})$ of 3.6 ppm. The NMR data associated with this latter species hint at the presence of a bridging Zr-CH_3-$B(C_6F_5)_3$ moiety, corresponding to the zwitterionic [(Bn_2Cyclam)ZrMe($CH_3B(C_6F_5)_3$) (**11**); over time **11** converts to **10**.[4a,20]

The reaction of **2** with $B(C_6F_5)_3$ was also done in d_8-THF. The formation of the solvent-stabilized cationic species [(Bn_2Cyclam)ZrMe(THF)][$B(C_6F_5)_3(CH_3)$] (**12**) was confirmed by ^{11}B and ^{19}F NMR spectroscopy. The resonance assigned to the zirconium-bound methyl group appears at 0.23 ppm as a singlet in the ^{1}H NMR spectrum, whereas the signal corresponding to the boron-bound methyl group appears at 0.51 ppm as a broad peak. In the $^{13}C\{^{1}H\}$ NMR spectrum, the latter is observed at 10.2 ppm, while the former is characterized by a resonance at 41.3 ppm.

The addition of one equivalent of $B(C_6F_5)_3$ to **2** was performed in d_8-toluene to assess the role of a less coordinating solvent. Upon mixing of the reagents and heating the NMR tube to −80 °C, a yellow oil precipitates out of solution. The NMR spectra at this temperature are inconclusive, as only weak signals are observed. At room temperature, although the precipitate did not dissolve completely, the ^{19}F NMR spectrum reveals the formation of $[B(C_6F_5)_3(CH_3)]^-$, suggesting that a solvent-stabilized zirconium cation [(Bn_2Cyclam)-ZrMe(Tol)][$B(C_6F_5)_3(CH_3)$] (**13**) is present in solution. As pointed out earlier, the formation of a cationic compound is also revealed by the AB system assigned to the benzylic group that is shifted upfield (3.32 and 3.17 ppm vs 4.53 and 4.35 ppm in **13** and **2**, respectively). The proton and carbon NMR spectra of the macrocycle are diagnostic of an average C_2 symmetry. [(Bn_2Cyclam)ZrMe(Tol)][$B(C_6F_5)_3(CH_3)$] is much less stable than the other solvent-stabilized cations obtained in dichloromethane and THF; along with methane formation, a new complex starts to form in solution. The ^{19}F NMR of this sample after one week at room temperature shows the presence of **13**, and a new species that was identified as (Bn_2Cyclam)$Zr(C_6F_5)(CH_2B(C_6F_5)_2)$ (**14**) formed upon methane elimination (see DFT results below). The identification of **14** was based on characteristic ^{19}F and ^{11}B NMR resonances. In the ^{19}F NMR spectrum there are two sets of resonances corresponding to two different C_6F_5 environments: the one of the Zr-(C_6F_5) group appears at −119.0, −150.4, and −158.9 ppm, whereas the signals assigned to the boron-bound C_6F_5 groups appear at −135.6, −160.6, and −164.7 ppm. The ^{11}B NMR spectrum shows a resonance at 86.6 ppm; this is in accordance with the expected trigonal-planar geometry around boron. The ZrCH_2B group was identified in the ^{1}H NMR spectrum by a signal at 5.80 ppm, which shows a correlation to a carbon at 100.5 ppm.[21] In summary, taking into account the existence of (i) two sets of resonances in the ^{19}F NMR, (ii) a trigonal-planar geometry around boron, which is bound to a methylenic group, and (iii) the identification of signals corresponding to a Zr-CH_2B group and methane in the ^{1}H NMR, all data support the formulation of this compound as **14**.

DFT Calculations. The reaction of the dimethyl complex [(Bn_2Cyclam)$_2$ZnMe_2] (**2**) with $B(C_6F_5)_3$ was studied by means of DFT calculations[22] (see Computational Details) and the calculated free energy profiles are presented in Figures 3 and 4.

The mechanism represented in Figure 3 starts with the pair of reagents, **2** and $B(C_6F_5)_3$, labeled **A** in the profile. In **A**, two independent molecules are present with a B−C_{Me} separation of 3.58 Å. In the first step of the mechanism one methyl is transferred from zirconium to boron, resulting in an inner-sphere ion pair,[23] [{(Bn_2Cyclam)ZrMe}$^+${(CH_3)-$B(C_6F_5)_3$}$^-$] (**B**). The Zr−C_{Me} distance in **B** (2.76 Å) is only slightly longer than the corresponding distances in the zwitterionic species taken from the Cambridge Structural Data Base,[24] which spread over a range of 2.47−2.67 Å. The long Zr−C_{Me} distance in **B** is associated with a weak interaction, as denoted by a Wiberg index (WI)[25] of 0.16. It should be noticed that **B** corresponds to the minor species

(20) Zuccaccia, C.; Stahl, N. G.; Macchioni, A.; Chen, M.-C.; Roberts, J. A.; Marks, T. J. *J. Am. Chem. Soc.* **2004**, *126*, 1448–1464.

(21) (a) Wondimagegn, T.; Xu, Z.; Vanka, K.; Ziegler, T. *Organometallics* **2004**, *23*, 3847–3852. (b) Gauvin, R. M.; Mazet, C.; Kress, J. *J. Organomet. Chem.* **2002**, *658*, 1–8. (c) Yue, N.; Hollink, E.; Guerin, F.; Stephan, D. W. *Organometallics* **2001**, *20*, 4424–4433. (d) Woodman, T. J.; Thornton-Pett, M.; Hughes, D. L.; Bochmann, M. *Organometallics* **2001**, *20*, 4080–4091. (e) Woodman, T. J.; Bochmann, M.; Thornton-Pett, M. *Chem. Commun.* **2001**, 329–330. (f) Karl, J.; Erker, G.; Froehlich, R. *J. Am. Chem. Soc.* **1997**, *119*, 11165–11173.

(22) Miehlich, B.; Savin, A.; Stoll, H.; Preuss, H. *Chem. Phys. Lett.* **1989**, *157*, 200–206.

(23) (a) Clot, E. *Eur. J. Inorg. Chem.* **2009**, 2319–2328. (b) Song, F.; Lancaster, S. J.; Cannon, R. D.; Schormann, M.; Humphrey, S. M.; Zuccaccia, C.; Macchioni, A.; Bochmann, M. *Organometallics* **2005**, *24*, 1315–1328. (c) Macchioni, A. *Chem. Rev.* **2005**, *105*, 2039–2073.

(24) Allen, F. H. *Acta Crystallogr.* **2002**, *B58*, 380.

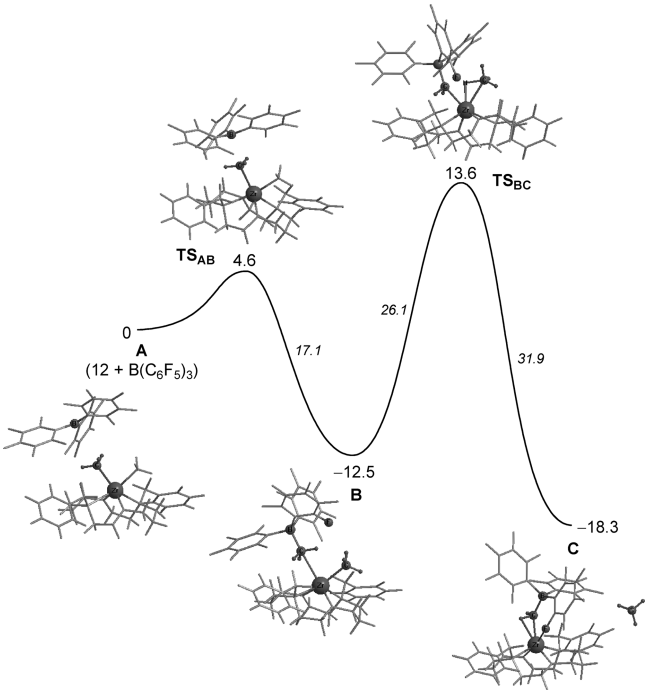

Figure 3. Free energy profile calculated (PBE1PBE) for methane elimination from $[(Bn_2Cyclam)_2ZnMe_2]$ (**2**) and $B(C_6F_5)_3$. The minima and the transition states were optimized, and the corresponding structures are represented with the relevant parts highlighted, in each step. Free energy values (kcal/mol) are referred to the pair of reactants (**A**), and energy barriers are presented in italics.

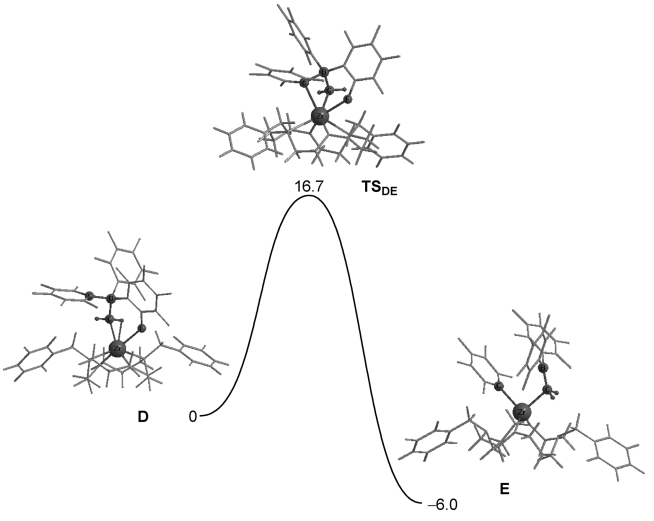

Figure 4. Free energy profile calculated (PBE1PBE) for the formation of $[(Bn_2Cyclam)Zr(C_6F_5)CH_2B(C_6F_5)_2]$ (**E**). The minima and the transition state were optimized, and the corresponding structures are represented with the relevant parts highlighted. Free energy values (kcal/mol) are referenced to the reactant $[(Bn_2Cyclam)Zr\{B(C_6F_5)_3(CH_2)\}]$ (**D**).

(**11**) that was detected in the ^{19}F NMR spectrum when the reaction was carried out in CD_2Cl_2 at low temperature, and it can be seen as the precursor of complex **10**, **12**, or **13** in the absence of a solvent molecule, as is the case in the model used for the calculations. In solution, the anion is expected to be readily displaced by the solvent, leading to a solvent-stabilized cationic complex. At the transition state, $\mathbf{TS_{AB}}$, the methyl transfer from Zr to B is only incipient. The $Zr-C_{Me}$ bond is only slightly longer (2.42 Å) and weaker (WI = 0.42) than the corresponding one in the reagent **A** (d_{Zr-C} = 2.32 Å, WI_{B-C} = 0.57), and it is still far from the values observed in the ion pair **B** (see above). Simultaneously, the new $B-C_{Me}$ bond is only starting to be formed, as shown by the long boron−carbon distance (2.43 Å) and by the WI of 0.33, which alludes to a weak interaction. The free energy barrier calculated for the first step (4.6 kcal/mol) denotes an easy process that is also favorable from the thermodynamic point of view (ΔG = −12.5 kcal/mol).

In the second step of the mechanism there is methane elimination from the ion pair **B** with formation of an unsaturated complex, $[(Bn_2Cyclam)Zr\{(CH_2)B(C_6F_5)_3\}]$, as shown in **C**. In the former complex the coordination of the borate is accomplished by the methylene C atom, as revealed by the corresponding bond distance and Wiberg index (d_{Zr-C} = 2.18 Å, WI = 0.80), but it is further reinforced by a Zr−F interaction and by a C−H agostic bond,[26] in order to compensate for a coordinatively unsaturated Zr(IV) metal center. The Zr−F bond in this complex corresponds to a moderately strong interaction (d_{Zr-F} = 2.56 Å, WI = 0.17), and the C−H agostic bond is characterized by a short Zr−H distance (2.24 Å) and a Wiberg index of 0.09.

At the transition state $\mathbf{TS_{BC}}$, both the $Zr-C_{Me}$ bond cleavage (d_{Zr-C} = 2.55 Å, WI = 0.35) and the formation of the new C−H bond (d_{C-H} = 1.37 Å, WI = 0.49) are already evident; yet these values are still far from the ones existing in **C**, where methane is displaced from the metal (d_{Zr-C} = 7.47 Å) and formation of the C−H bond is accomplished (d_{C-H} = 1.09 Å, WI = 0.93). More importantly, the H transfer from $B(C_6F_5)_3(CH_3)^-$ to CH_3 is a process assisted by the metal, since in $\mathbf{TS_{BC}}$ the H atom involved in the transfer is weakly bonded to Zr, as shown by a short Zr−H length of 1.98 Å and a significant interaction with WI_{Zr-H} = 0.10. The second step of the calculated mechanism is thermodynamically favored (ΔG = −5.8 kcal/mol) and presents a moderate energy barrier of 26.1 kcal/mol, which, being the highest of the entire path, indicates methane elimination as the reaction rate-limiting step.

The final step of the mechanism corresponds to an intramolecular rearrangement of complex $[(Bn_2Cyclam)Zr\{(CH_2)B(C_6F_5)_3\}]$ (**D**) giving the final product $(Bn_2Cyclam)Zr(C_6F_5)(CH_2B(C_6F_5)_2)$ (**E**). The free energy profile associated with this process is depicted in Figure 4. It should be highlighted that the difference between **C** and **D** is that in the former there is a methane molecule, while the latter only comprises the complex $[(Bn_2Cyclam)Zr\{(CH_2)B(C_6F_5)_3\}]$.

In the process depicted in Figure 4, the system goes from one unsaturated complex (**D**) to a six-coordinated complex with two new anionic ligands, $C_6F_5^-$ and $CH_2B(C_6F_5)_2^-$. In other words, it corresponds to the transfer of one pentafluorophenyl group from boron to the metal. In this compound, the new Zr−C bond distances are 2.34 and 2.35 Å, for $Zr-C_{C_6F_5}$ and $Zr-C_{CH_2B(C_6F_5)_2}$, respectively, and the corresponding Wiberg indices are 0.49 and 0.48, respectively. At the transition state, $\mathbf{TS_{D-E}}$, $B-C_{C_6F_5}$ bond breaking is manifested

(25) (a) Wiberg, K. B. *Tetrahedron* **1968**, *24*, 1083–1096. (b) Wiberg indices are electronic parameters related to the electron density between atoms. They can be obtained from a natural population analysis and provide an indication of the bond strength.

(26) Brookhart, M.; Green, M. L. H.; Parkin, G. *Proc. Natl. Acad. Sci. U. S. A.* **2007**, *104*, 6908−6914.

by a weak B−$C_{C_6F_5}$ interaction (d_{B-C} = 2.00 Å, WI = 0.52). Conversely, formation of the new Zr−$C_{C_6F_5}$ is well advanced, with a Zr−$C_{C_6F_5}$ distance of 2.69 Å and a Wiberg index of 0.24, indicating a significant interaction. It should be noted that until the formation of the new Zr−$C_{C_6F_5}$ bond the metal center remains unsaturated, and thus, at the transition state $\mathbf{TS_{D-E}}$, where this bond is not yet completely formed, there is one Zr−F interaction, similar to one present in **D**. This interaction involves one F atom of a pentafluorophenyl group that remains bonded to boron and stabilizes $\mathbf{TS_{D-E}}$ by providing extra electron density to the electron-deficient Zr(IV) center. The reaction from **D** to **E** is favorable from the thermodynamic point of view (ΔG = −6.0 kcal/mol) and has an accessible energy barrier of 16.7 kcal/mol.

The calculations indicate a plausible path for the formation of (Bn_2Cyclam)Zr(C_6F_5)($CH_2B(C_6F_5)_2$) (**E**) with methane elimination as the rate-determining step. **E** corresponds to species **14** and was identified by NMR as the final product of the reaction of the dimethyl complex (Bn_2Cyclam)$_2$ZrMe_2 (**2**) with $B(C_6F_5)_3$.

Concluding Remarks

In summary, a series of zirconium alkyl complexes that incorporate a saturated tetraazamacrocycle ancillary ligand were prepared. Variation on the alkyl ligands induces different geometry around the metal center; such changes are dictated by the steric bulk of the ligands that occupy the remaining coordination positions and are intimately related to the flexibility of the dianionic cyclam ligand. This behavior has already been observed in analogous complexes supported by this ligand set.

The stability of the alkyl complexes was assessed, and it was found that C−H activation of the benzyl groups of the macrocycle occurs with concomitant alkane elimination; this process occurs both in solution and in the solid state. The bis(*ortho*-metalated) complex reacts with HCCPh to regenerate the ancillary ligand and two phenylacetylide ligands. These results indicate that the *ortho*-metalation reaction and the Zr−C bond formation may be reversible and raise the expectation of exploring both the reactivity of the *ortho*-metalated species and its potential in catalytic processes.

Reactions of the bis(alkyl) complexes with $B(C_6F_5)_3$ generate cationic derivatives upon abstraction of one alkyl ligand. The structure and coordination around the zirconium metal center are solvent and alkyl-ligand dependent. This is well illustrated in two examples. In the zirconium-benzyl cation, the benzyl ligand is η^2-ligated in noncoordinating solvents, whereas in the presence of a coordinating solvent such as THF it displays the η^1-coordination mode. In the zirconium-methyl cation case, whereas it is stable in dichloromethane or THF solutions, it shows a different behavior in toluene. In the latter case, the transfer of a pentafluoro group to zirconium is observed. This rearrangement involves the cleavage of one B−C_6F_5 bond and the C−H activation of a bridging methyl group of an intermediate zwitterionic complex. DFT studies provided a plausible mechanism for this reaction, indicating methane elimination as the rate-determining step.

Preliminary studies with dichloro complexes supported by this ligand set, in the presence of MAO in toluene, have shown them to be moderately active as precatalysts for the polymerization of ethylene. Motivated by the stability of the cationic complexes in solution, we are now interested in evaluating their competence in the polymerization of olefins.

Experimental Section

General Considerations. Unless otherwise stated, all manipulations were performed under an atmosphere of dry oxygen-free dinitrogen by means of standard Schlenk and glovebox techniques. Solvents were predried using 4 Å molecular sieves, refluxed over sodium-benzophenone (diethyl ether, toluene, THF) or CaH_2 (*n*-hexane) under an atmosphere of N_2, and collected by distillation. Deuterated solvents were dried with 4 Å molecular sieves and freeze−pump−thaw degassed prior to use. Proton and carbon NMR spectra were recorded in a Bruker AVANCE 300 or 400 MHz, at 296 K unless stated otherwise, referenced internally to residual proton-solvent (^{1}H) or solvent (^{13}C) resonances, and reported relative to tetramethylsilane (0 ppm). Elemental analyses were obtained from Laboratório de Análises do IST, Lisbon, Portugal, and were also performed in the departmental facility of the University of British Columbia. The compounds (Bn_2Cyclam)ZrCl_2[5b] and $B(C_6F_5)_3$[27] were prepared according to described procedures. All other reagents were commercial grade and used without further purification.

(Bn_2Cyclam)Zr$(Me)_2$ (2). To a THF suspension of (Bn_2-Cyclam)ZrCl_2 (0.31 g, 0.58 mmol) at −10 °C was slowly added 0.54 mL of a MgClMe solution (2.18 M in THF). After a while the suspension completely dissolved and the light yellow solution started to become colorless. The mixture was allowed to come to room temperature, and it reacted for further 3 h. The solvent was evaporated and the light beige residue was extracted with 15 mL of toluene. To the toluene extract was added 0.2 mL of dioxane, and the suspension was filtered and taken to dryness. The solid was washed with cold hexanes and stored at −20 °C (0.16 g, 63%). ^{1}H NMR (C_6D_6, 300.1 MHz, 296 K): δ (ppm) 7.20−7.10 (br, 10H, *H*-Ph), 4.54 (d, 2H, $^2J_{HH}$ = 14 Hz, PhCH_2N), 4.35 (d, 2H, $^2J_{HH}$ = 14 Hz, PhCH_2N), 4.00 (m, 2H, [C3]NCH_2), 3.62 (m, 2H, [C2]NCH_2), 2.91 (m, 2H, [C3]NCH_2), 2.75−2.54 (overlapping, 6H total, 2H, [C3]NCH_2, 4H, [C2]NCH_2), 2.26 (m, 2H, [C3]NCH_2), 2.15 (m, 2H, [C2]NCH_2), 1.49 (m, 2H, CH_2-C$H_2$$CH_2$), 1.02 (m, 2H, CH_2C$H_2$$CH_2$), 0.58 (s, 6H, ZrC$H_3$). ^{13}C{^{1}H} NMR ($C_6D_6$, 75.5 MHz, 296 K): δ (ppm) 133.0 (*i*-Ph), 132.7 (*o*-Ph), 128.1, 127.9 (*m*-Ph and *p*-Ph), 56.5 (PhCH_2N), 55.9 ([C3]NCH_2), 52.3 ([C2]NCH_2), 50.9 ([C3]NCH_2), 49.9 ([C2]NCH_2), 36.5 (ZrCH_3), 24.8 ($CH_2CH_2CH_2$). ^{1}H NMR (CD_2Cl_2, 400.1 MHz, 296 K): δ (ppm) 7.38−7.34 (overlapping, 10H, *H*-Ph), 4.55 (d, 2H, $^2J_{HH}$ = 14 Hz, PhCH_2N), 4.26 (d, 2H, $^2J_{HH}$ = 14 Hz, PhCH_2N), 3.84−3.72 (overlapping, 4H total, 2H, [C3]NCH_2, 2H, [C2]NCH_2), 3.05−2.96 (overlapping, 6H total, 2H, [C3]NCH_2, 4H, [C2]NCH_2), 2.77 (m, 2H, [C3]NCH_2), 2.49−2.39 (overlapping, 4H total, 2H, [C3]NCH_2, 2H, [C2]NCH_2), 1.82 (m, 2H, CH_2C$H_2$$CH_2$), 1.34 (m, 2H, CH_2C$H_2$$CH_2$), −0.14 (s, 6H, ZrC$H_3$). ^{13}C{^{1}H} NMR ($CD_2Cl_2$, 100.6 MHz, 296 K): δ (ppm) 133.3 (*i*-Ph), 132.9 (*o*-Ph), 128.6 (*p*-Ph), 128.5 (*m*-Ph), 56.9 (PhCH_2N), 55.9 ([C3]NCH_2), 52.3 ([C2]NCH_2), 50.7 ([C3]NCH_2), 50.3 ([C2]NCH_2), 34.5 (ZrCH_3), 24.8 ($CH_2CH_2CH_2$). Satisfactory elemental analysis was not possible due to thermal instability of the product.

(Bn_2Cyclam)Zr$(CH_2Ph)_2$ (3). To a THF suspension of (Bn_2-Cyclam)ZrCl_2 (0.39 g, 0.70 mmol) at −10 °C was slowly added 0.88 mL of a MgClCH_2Ph solution (1.64 M in diethyl ether). The suspension completely dissolved after 1 h. The mixture was allowed to come to room temperature, and it reacted for a further 3 h. The solution was taken to dryness, and the yellow residue was extracted with 10 mL of toluene. The toluene extract was concentrated, and 0.2 mL of dioxane was added. The suspension was filtered and evaporated to dryness. The yellow solid obtained in 80% yield (0.36 g) was stored at −20 °C. Crystals suitable for X-ray diffraction were obtained from a concentrated toluene solution. ^{1}H NMR (C_6D_6, 400.1 MHz, 296 K): δ (ppm) 7.44 (m, 4H, *o*-PhCH_2Zr), 7.29 (m, 4H, *m*-PhCH_2Zr), 7.18−7.11 (overlapping, 6H total, 4H, *m*-PhCH_2N, 2H, *p*-PhCH_2N),

(27) Massey, A. G.; Park, A. J. *J. Organomet. Chem.* **1964**, *2*, 245–250.

7.01−6.92 (overlapping, 6H total, 2H, *p*-PhCH_2Zr, 4H, *o*-PhCH_2N), 4.37 (d, 2H, $^2J_{HH}$ = 14 Hz, PhCH_2N), 3.51 (d, 2H, $^2J_{HH}$ = 14 Hz, PhCH_2N), 3.05 (m, 2H, [C3]NCH_2), 2.87 (overlapping, 6H total, 2H, [C3]NCH_2, 4H, [C2]NCH_2), 2.72 (d, 2H, $^2J_{HH}$ = 9 Hz, PhCH_2Zr), 2.63 (d, 2H, $^2J_{HH}$ = 9 Hz, PhCH_2Zr), 2.38 (m, 4H, [C3]NCH_2), 2.19 (m, 2H, $CH_2CH_2CH_2$), 2.08 (m, 2H, [C2]NCH_2), 2.00 (m, 2H, [C2]NCH_2), 1.48−1.37 (br, 2H, $CH_2CH_2CH_2$). $^{13}C\{^1H\}$ NMR (C_6D_6, 100.6 MHz, 296 K): δ (ppm) 150.6 (*i*-PhCH_2Zr), 132.9 (*i*-PhCH_2N), 132.7 (*o*-PhCH_2N), 130.1 (*o*-PhCH_2Zr), overlapping with C_6D_6 (*m*-PhCH_2N, *p*-PhCH_2N, *m*-PhCH_2Zr), 119.7 (*p*-PhCH_2Zr), 66.1 (PhCH$_2$Zr), 60.3 (PhCH_2N), 59.1 ([C3]NCH_2), 55.6 ([C2]NCH_2), 55.2 ([C2]NCH_2), 49.6 ([C3]NCH_2), 26.1 ($CH_2CH_2CH_2$). ^1H NMR (CD_2Cl_2, 300.1 MHz, 296 K): δ (ppm) 7.33−7.31 (overlapping, 6H total, 4H, *m*-PhCH_2N, 2H, *p*-PhCH_2N), 7.25−7.15 (overlapping, 8H total, 4H, *o*-PhCH_2Zr, 4H, *m*-PhCH_2Zr), 7.07 (m, 4H, *o*-PhCH_2N), 6.86 (m, 2H, *p*-PhCH_2Zr), 4.40 (d, 2H, $^2J_{HH}$ = 14 Hz, PhCH_2N), 3.39 (d, 2H, $^2J_{HH}$ = 14 Hz, PhCH_2N), 3.13−2.89 (overlapping, 6H total, 4H, [C3]NCH_2, 2H, [C2]NCH_2), 2.76 (m, 2H, [C2]NCH_2), 2.67−2.33 (overlapping, 6H total, 4H, [C3]NCH_2, 2H, $CH_2CH_2CH_2$), 2.41 (d, 2H, $^2J_{HH}$ = 8 Hz, PhCH_2Zr), 2.35 (d, 2H, $^2J_{HH}$ = 8 Hz, PhCH_2Zr), 2.02−1.82 (overlapping, 6H total, 4H, [C2]NCH_2, 2H, $CH_2CH_2CH_2$). $^{13}C\{^1H\}$ NMR (CD_2Cl_2, 75.5 MHz, 296 K): δ (ppm) 150.8 (*i*-PhCH_2Zr), 133.1 (*i*-PhCH_2N), 132.9 (*o*-PhCH_2N), 129.8 (*o*-PhCH_2Zr), 128.7 (*p*-PhCH_2N), 128.4 (*m*-PhCH_2N), 128.0 (*m*-PhCH_2Zr), 119.6 (*p*-PhCH_2Zr), 64.9 ($^1J_{CH}$ = 124 Hz, PhCH$_2$Zr), 60.4 (PhCH_2N), 59.3 ([C3]NCH_2), 55.7 ([C2]NCH_2), 55.1 ([C2]NCH_2), 49.9 ([C3]NCH_2), 26.4 ($CH_2CH_2CH_2$). Anal. Calcd for $C_{38}H_{48}N_4Zr(C_7H_8)$: C 72.63, H 7.58, N 7.53. Found: C 73.02, H 7.43, N 7.49.

(Bn$_2$Cyclam)Zr(^{n}Bu)$_2$ (4). To a THF suspension of (Bn$_2$-Cyclam)ZrCl_2 (1.08 g, 2.0 mmol) at −30 °C was slowly added 2.5 mL of a LiBu^n solution (1.6 M in hexanes). After a while the suspension started to dissolve and the light yellow solution turned yellowish-brown. The mixture reacted for a further 2 h, and the solvent was evaporated. The residue was extracted with 15 mL of toluene. The solvent was evaporated to yield 1.0 g of **4** (86%). The solid was redissolved in diethyl ether and stored at −20 °C. Crystalline material suitable for X-ray diffraction was obtained from this diethyl ether solution. ^1H NMR (C_6D_6, 400.1 MHz, 296 K): δ (ppm) 7.15−7.05 (br, 10H, *H*-Ph), 4.65 (d, 2H, $^2J_{HH}$ = 14 Hz, PhCH_2N), 4.39 (d, 2H, $^2J_{HH}$ = 14 Hz, PhCH_2N), 3.85 (m, 2H, [C3]CH_2N), 3.69 (m, 2H, [C2]CH_2N), 2.98 (m, 2H, [C3]CH_2N), 2.75 (m, 2H, [C3]CH_2N), 2.72−2.57 (overlapping, 4H total, 2H, [C2]CH_2N and 2H, [C2]CH_2N), 2.27−2.13 (overlapping, 8H total, 4H, ZrCH$_2$CH_2CH$_2$, 2H, [C3]CH_2N and 2H, [C2]CH_2N), 1.81 (m, 4H, ZrCH$_2$CH$_2$CH_2), 1.48 (m, 2H, CH$_2$CH_2CH$_2$), 1.25 (m, 6H, Zr(CH$_2$)$_3$CH_3), 1.10−0.99 (overlapping, 4H total, 2H, ZrCH_2CH$_2$ and 2H, CH$_2$CH_2CH$_2$), 0.60 (m, 2H, ZrCH_2CH$_2$). $^{13}C\{^1H\}$ NMR (C_6D_6, 100.6 MHz, 296 K): δ (ppm) 132.7 (*o*-Ph), 132.0 (*i*-Ph), 128.2 and 128.0 (overlapping with C_6D_6, *m*-Ph and *p*-Ph), 58.2 (ZrCH$_2$CH$_2$), 56.1 (PhCH$_2$N), 55.9 ([C3]CH$_2$N), 53.0 ([C2]CH$_2$N), 51.8 ([C3]CH$_2$N), 50.9 ([C2]CH$_2$N), 32.9 (ZrCH$_2$CH$_2$CH$_2$), 31.4 (ZrCH$_2$CH$_2$CH$_2$), 25.4 (CH$_2$CH$_2$CH$_2$), 14.7 (Zr(CH$_2$)$_3$CH$_3$). Anal. Calcd for $C_{32}H_{52}N_4Zr$: C 65.81, H 8.97, N 9.59. Found: C 65.66, H 8.67, N 9.60.

(Bn$_2$Cyclam)Zr(CCPh)$_2$ (5). To a THF suspension of (Bn$_2$-Cyclam)ZrCl_2 (0.38 g, 0.71 mmol) was slowly added 1.6 mL of a LiCCPh solution (1.0 M in THF). After a while the suspension started to dissolve and the light yellow solution turned orange. The mixture reacted for a further 12 h, and the solvent was evaporated. The oily residue was extracted with 15 mL of toluene. After taking the extract to dryness, diethyl ether was added to remove a brown impurity. The solution was again taken to dryness and washed with minimal hexanes to give a yellow solid in 52% yield (0.25 g). ^1H NMR (C_6D_6, 400.1 MHz, 296 K): δ (ppm) 7.71 (d, 4H, *o*-PhCCZr), 7.21−7.11 (overlapping, 10H total, *H*-PhCH$_2$N), 7.06−7.00 (overlapping, 6H, *H*-PhCCZr), 5.42 (d, 2H, $^2J_{HH}$ = 14 Hz, PhCH_2N), 4.73 (m, 2H, [C3]CH_2N), 4.40 (d, 2H, $^2J_{HH}$ = 14 Hz, PhCH_2N), 3.69 (m, 2H, [C3]CH_2N), 3.60 (m, 2H, [C2]CH_2N), 2.84 (m, 2H, [C2]CH_2N), 2.74−2.68 (overlapping, 4H total, 2H [C3]CH_2N, 2H [C2]CH_2N), 2.43 (m, 2H, [C3]CH_2N), 2.17 (m, 2H, [C2]CH_2N), 1.61−1.51 (br, 2H, $CH_2CH_2CH_2$), 1.17 (m, 2H, $CH_2CH_2CH_2$). $^{13}C\{^1H\}$ NMR (C_6D_6, 100.6 MHz, 296 K): δ (ppm) 150.7 (PhC*C*Zr), 133.4 (*i*-PhCH$_2$N), 133.2 (*Ph*CH$_2$N), 132.3 (*o*-PhCCZr), 128.9, 128.5, 128.3 (*Ph*CH$_2$N and *Ph*CCZr), 127.7 (*i*-PhCCZr), 126.8 (*Ph*CH$_2$N or *Ph*CCZr), 106.3 (PhCCZr), 57.6 (PhCH$_2$N), 57.1 ([C3]CH$_2$N), 53.4 ([C2]CH$_2$N), 52.8 ([C3]CH$_2$N), 49.8 ([C2]CH$_2$N), 25.6 ($CH_2CH_2CH_2$). IR: 2069 cm^{-1} (C≡C stretching). Anal. Calcd for $C_{40}H_{44}N_4Zr$: C 71.49, H 6.60, N 8.34. Found: C 69.91, H 6.74, N 7.47.

((C$_6$H$_4$CH$_2$)$_2$Cyclam)Zr (6). A C_6D_6 solution of **2** or **4** in a NMR tube was heated at 70 °C over a period of 2 h. On the basis of the ^1H NMR spectrum, the conversion was complete. Alternatively, a Schlenk was charged with **4** (0.80 g, 1.36 mmol) and heated at 70 °C for 2 days, obtaining **6** quantitatively. Starting from complex **3**, the reaction was monitored by NMR, and complete conversion was achieved over a period of 72 h under mild reflux of the C_6D_6 solution. ^1H NMR (C_6D_6, 400.1 MHz, 296 K): δ (ppm) 8.20 (m, 2H, *H*(*6*)-Ph) 7.30−7.10 (overlapping, 6H total, 2H, *H*(*3*)-Ph, 2H, *H*(*4*)-Ph, 2H, *H*(*5*)-Ph), 4.81 (d, 2H, $^2J_{HH}$ = 14 Hz, PhCH_2N), 3.60 (m, 2H, [C2]CH_2N), 3.23 (m, 2H, [C3]CH_2N), 3.02 (m, 2H, [C2]CH_2N), 2.84 (d, 2H, $^2J_{HH}$ = 14 Hz, PhCH_2N), 2.82 (m, 2H, [C3]CH_2N), 2.62 (m, 2H, [C2]CH_2N), 2.28 (m, 2H, [C3]CH_2N), 2.07 (overlapping, 4H total, 2H, [C2]CH_2N, 2H, [C3]CH_2N), 1.39 (m, 2H, CH$_2$CH_2CH$_2$), 0.89 (m, 2H, CH$_2$CH_2CH$_2$). $^{13}C\{^1H\}$ NMR (C_6D_6, 100.6 MHz, 296 K): δ (ppm) 188.5 (*C*(*1*)-Ph), 151.1 (*C*(*2*)-Ph), 140.8 (*C*(*6*)-Ph), 126.8, 125.4, 124.1 (*C*(*3*)-Ph, (*C*(*4*)-Ph, (*C*(*5*)-Ph), 63.3 (PhCH$_2$N), 59.7 ([C3]CH$_2$N), 55.4 ([C2]CH$_2$N), 52.9 ([C2]CH$_2$N), 50.0 ([C3]CH$_2$N), 26.4 (CH$_2$CH$_2$CH$_2$). MS (ESI): *m*/*z* 466. A *m*/*z* of 466 is also observed when **2** is analyzed, indicative of how thermally sensitive and prone to decomposition complex **2** is. Anal. Calcd for $C_{24}H_{32}N_4Zr$: C 61.62, H 6.90, N 11.98. Found: C 61.83, H 7.16, N 11.63.

((C$_6$H$_4$CH$_2$)BnCyclam))Zr(CCPh) (7). One equivalent of HCCPh (5 mg, 0.05 mmol) was added to a solution of **6**, obtained *in situ* by heating a C_6D_6 solution of **2** (0.03 g, 0.05 mmol). After 18 h at room temperature, the ^1H NMR spectrum showed a set of resonances corresponding to compound **7** (about 38%) and to compound **5**. Full assignment of the aromatic resonances was not possible due to the complexity of the ^1H and ^{13}C spectra. ^1H NMR (C_6D_6, 400.1 MHz, 296 K): δ (ppm) 8.97 (d, 1H, *H*(*6*)-Ph), 5.31 (d, 1H, $^2J_{HH}$ = 14 Hz, PhCH_2N), 4.77−4.67 (overlapping with **5**, 1H, PhCH_2N), 4.51 (d, 1H, $^2J_{HH}$ = 14 Hz, PhCH_2N), 4.18 (m, 1H, CH_2N), 3.37 (overlapping, 2H total, 1H, CH_2N and, 1H, CH_2N), 3.11−2.96 (overlapping with **2**, 2H total, 1H, CH_2N and, 1H, PhCH_2N), 2.88−2.67 (overlapping with **6** and **5**, 5H, CH_2N), 2.53−2.41 (overlapping with **5**, 5H, CH_2N), 2.32−2.19 (overlapping with **6** and **5**, 1H, CH_2N), 2.11−2.05 (overlapping with **6** and **5**, 1H, CH_2N), 1.63−1.37 (overlapping with **6** and **5**, 2H, CH$_2$CH_2CH$_2$), 1.19−1.15 (overlapping with **6**, 1H, CH$_2$CH_2CH$_2$), 0.86−0.82 (overlapping with **6**, 1H, CH$_2$CH_2CH$_2$). $^{13}C\{^1H\}$ NMR (C_6D_6, 100.6 MHz, 296 K): δ (ppm) 188.3 (*C*(*1*)-Ph), 150.4 (PhC*C*Zr), 150.1 (*C*(*2*)-Ph), 142.2 (*C*(*6*)-Ph), 134.3, 133.1, 133.0, 132.3, 132.2, 129.7, 128.9, 127.8, 127.3, 126.7, 125.7, 125.6, 124.2 (*Ph*CH$_2$N, *Ph*CCZr, *C*(*3*)-Ph, *C*(*4*)-Ph, *C*(*5*)-Ph), 63.9 (PhCH$_2$N), 58.7 (PhCH$_2$N), 58.7 (CH$_2$N), 57.1 (CH$_2$N), 56.0 (CH$_2$N), 54.7 (CH$_2$N), 52.1 (CH$_2$N), 51.1 (CH$_2$N), 49.5 (CH$_2$N), 48.5 (CH$_2$N), 24.9 (CH$_2$CH$_2$CH$_2$), 24.5 (CH$_2$CH$_2$CH$_2$).

[(Bn$_2$Cyclam)Zr(η^2-CH$_2$Ph)][PhCH$_2$B(C$_6$F$_5$)$_3$] (8). Method A1: At room temperature, a J-Young NMR tube was charged with complex **3** (0.03 g, 0.05 mmol) and B(C_6F_5)$_3$ (0.02 mg, 0.05 mmol), and approximately 0.5 mL of CD_2Cl_2 was added to the mixture, leading to the formation of a light yellow solution. NMR shows the conversion was complete after 15 min. Method A2: To a solution of complex **3** (0.31 g, 0.47 mmol) in dichloromethane was added a solution of B(C_6F_5)$_3$ (0.24 g, 0.47 mmol) in

the same solvent. The mixture was stirred overnight at room temperature. Evaporation of the solvent afforded **8** as a yellow solid in quantitative yield. ^{1}H NMR (CD_2Cl_2, 300.1 MHz, 296 K): δ (ppm) 7.65 (m, 2H, *m*-PhCH_2Zr), 7.51−7.43 (overlapping, 7H total, 1H, *p*-PhCH_2Zr, 4H, *m*-PhCH_2N, 2H, *p*-PhCH_2N), 7.25 (m, 4H, *o*-PhCH_2N), 6.96 (m, 2H, *o*-PhCH_2Zr), 6.89 (m, 2H, *m*-PhCH_2B), 6.82−6.76 (overlapping, 3H total, 2H, *o*-PhCH_2B, 1H, *p*-PhCH_2B), 4.19 (d, 2H, $^2J_{HH}$ = 14 Hz, PhCH_2N), 3.88−3.67 (overlapping, 4H total, 2H, [C3]NCH_2, 2H, [C2]NCH_2), 3.21−2.82 (overlapping, 8H total, 4H, [C3]NCH_2, 4H, [C2]NCH_2), 3.08 (d, 2H, $^2J_{HH}$ = 14 Hz, PhCH_2N), 3.00 (d, 1H, $^2J_{HH}$ = 9 Hz, PhCH_2Zr), 2.86 (s, 2H, PhCH_2B), 2.74−2.60 (overlapping, 4H total, 2H, [C2]NCH_2, 2H, [C3]NCH_2), 2.70 (d, 1H, $^2J_{HH}$ = 9 Hz, PhCH_2Zr), 1.88−1.76 (br, 2H, $CH_2CH_2CH_2$), 1.65 (m, 2H, $CH_2CH_2CH_2$). ^{13}C{^{1}H} NMR (CD_2Cl_2, 75.5 MHz, 296 K): δ (ppm) 150.0 (BC_6F_5), 149.2 (*i*-PhCH_2B), 147.2 (BC_6F_5), 140.0 (BC_6F_5), 139.4 (*i*-PhCH_2Zr), 138.5 (BC_6F_5), 136.4 (BC_6F_5), 135.3 (BC_6F_5), 134.9 (*m*-PhCH_2Zr), 132.6 (*o*-PhCH_2N), 130.0 (*i*-PhCH_2N), 129.7 (*p*-PhCH_2N), 129.2 (*m*-PhCH_2N), 129.2 (*o*-PhCH_2B), 128.7 (*o*-PhCH_2Zr), 127.9 (*p*-PhCH_2Zr), 127.3 (*m*-PhCH_2B), 122.9 (*p*-PhCH_2B), 69.2 ($^1J_{CH}$ = 139 Hz, PhCH_2Zr), 57.3 ([C3]NCH_2), 56.6 (PhCH_2N), 51.5 ([C2]NCH_2), 51.1 ([C3]NCH_2), 49.5 ([C2]NCH_2), 32.0 (br, PhCH_2B), 24.6 ($CH_2CH_2CH_2$). ^{19}F NMR (CD_2Cl_2, 282.4 MHz, 296 K): δ (ppm) −131.2 (d, $^3J_{FF}$ = 23 Hz, F_o), −164.7 (t, $^3J_{FF}$ = 21 Hz, F_p), −167.5 (t, $^3J_{FF}$ = 19 Hz, F_m). ^{11}B NMR (CD_2Cl_2, 96.3 MHz, 296 K): δ (ppm) −12.9. MS (ESI): *m*/*z* 603.1 [PhCH_2B(C_6F_5)$_3$]$^-$. Anal. Calcd for $C_{56}H_{48}BF_{15}N_4Zr$: C 57.78, H 4.16, N 4.81. Found: C 57.88, H 4.58, N 4.39.

Method B: The reaction conditions were analogous to method A, but it was carried out in d_8-toluene. ^{1}H NMR (d_8-toluene, 500.1 MHz, 296 K): δ (ppm) 7.22−6.77 (overlapping, 20H total, *H*-Ph), 3.63 (d, 2H, $^2J_{HH}$ = 14 Hz, PhCH_2N), 3.39 (s, 2H, PhCH_2B), 3.27 (m, 2H, [C2]NCH_2), 3.13 (m, 2H, [C3]NCH_2), 2.60 (m, 2H, [C2]NCH_2), 2.53−2.41 (overlapping, 7H total, 2H, PhCH_2N, 1H, PhCH_2Zr, 2H, [C3]NCH_2, 2H, [C2]NCH_2), 2.21−2.16 (overlapping, 5H total, 1H, PhCH_2Zr, 2H, [C3]NCH_2, 2H, [C2]NCH_2), 2.11−2.05 (overlapping with d_8-toluene, 2H, [C3]NCH_2), 1.31−1.23 (br, 2H, $CH_2CH_2CH_2$), 1.05 (m, 2H, $CH_2CH_2CH_2$). ^{13}C{^{1}H} NMR (CD_2Cl_2, 125.8 MHz, 296 K): δ (ppm) 151.0 (*i*-PhCH_2B), 139.9 (*i*-PhCH_2Zr), 134.9 (*m*-PhCH_2Zr), 133.0 (*o*-PhCH_2N), 130.2 (*i*-PhCH_2N), 130.1−128.5 (overlapping with d_8-toluene, *p*-PhCH_2N, *m*-PhCH_2N, *o*-PhCH_2B, *o*-PhCH_2Zr), 128.3 (*p*-PhCH_2Zr), 126.5 (*m*-PhCH_2B), 124.0 (*p*-PhCH_2B), 69.3 ($^1J_{CH}$ = 138 Hz, PhCH_2Zr), 57.4 ([C3]-NCH_2), 56.9 (PhCH_2N), 51.5 ([C2]NCH_2), 51.2 ([C3]NCH_2), 49.4 ([C2]NCH_2), 32.0 (br, PhCH_2B), 24.7 ($CH_2CH_2CH_2$). The low solubility of this compound in d_8-toluene does not allow the clear identification of the carbon resonances for the pentafluorophenyl groups, as they are weak, and due to the coupling with ^{19}F, they show as broad multiplets ranging from 151 to 137 ppm. ^{19}F NMR (d_8-toluene, 282.4 MHz, 296 K): δ (ppm) −130.2 (d, $^3J_{FF}$ = 23 Hz, F_o), −164.0 (t, $^3J_{FF}$ = 21 Hz, F_p), −166.7 (t, $^3J_{FF}$ = 20 Hz, F_m). ^{11}B NMR (d_8-toluene, 96.3 MHz, 296 K): δ (ppm) −12.2.

[(Bn$_2$Cyclam)Zr(CH$_2$Ph)(THF)][PhCH$_2$B(C$_6$F$_5$)$_3$] (9). A vial was charged with **3** (0.03 g, 0.05 mmol) and dissolved in THF. A solution of B(C_6F_5)$_3$ (0.02 g, 0.05 mmol) was added dropwise, and the mixture was stirred overnight. It was then transferred to a J-Young tube, whose NMR indicated complete conversion. ^{1}H NMR (d_8-THF, 400.1 MHz, 296 K): δ (ppm) 7.40 (br, 10H total, *H*-Ph), 7.22 (m, 2H, BCH$_2$*Ph*), 7.11 (overlapping, 4H total, ZrCH$_2$*Ph*), 6.92 (m, 1H, ZrCH$_2$*Ph*), 6.75 (m, 2H, BCH$_2$*Ph*), 6.65 (m, 1H, BCH$_2$*Ph*), 4.66 (d, 2H, $^2J_{HH}$ = 14 Hz, PhCH_2N), 4.04 (d, 2H, $^2J_{HH}$ = 14 Hz, PhCH_2N), 3.97 (m, 2H, [C2]NCH_2), 3.66 (m, 2H, [C3]NCH_2), 3.19 (m, 2H, [C2]NCH_2), 3.05 (m, 2H, [C2]NCH_2), 2.95 (m, 2H, [C3]NCH_2), 2.85 (br, 2H, BCH_2Ph), 2.72 (m, 2H, [C3]NCH_2), 2.57 (m, 2H, [C3]NCH_2), 2.55 (d, 1H, $^2J_{HH}$ = 12 Hz, ZrCH_2Ph), 2.21 (d, 1H, $^2J_{HH}$ = 12 Hz, ZrCH_2Ph), 2.01 (m, 2H, $CH_2CH_2CH_2$), 1.57 (m, 2H, $CH_2CH_2CH_2$). ^{13}C{^{1}H} NMR (d_8-THF, 100.6 MHz, 296 K): δ (ppm) 150.3 (br, C_6F_5), 149.5 (*i*-PhCH$_2$B), 148.0 (br, C_6F_5), 147.1 (*i*-PhCH$_2$Zr), 139.4 (br, C_6F_5), 138.3 (br, C_6F_5), 137.1 (br, C_6F_5), 136.0 (br, C_6F_5), 133.3 (*Ph*CH$_2$N), 130.9 (*i*-PhCH$_2$N), 130.5 (*Ph*CH$_2$N), 129.7 (*Ph*CH$_2$N), 129.4, 128.9, 127.2, 123.7 (*Ph*), 122.9 (*Ph*CH$_2$Zr), 68.2 ($^1J_{CH}$ = 124 Hz, PhCH$_2$Zr), 57.5 (PhCH$_2$N), 57.3 ([C3]NCH$_2$), 54.7 ([C3]NCH$_2$), 53.6 ([C2]NCH$_2$), 51.0 ([C2]NCH$_2$), 32.2 (br, BCH$_2$Ph), 25.3 (CH$_2$CH$_2$CH$_2$). ^{19}F NMR (d_8-THF, MHz, 296 K): δ (ppm) −133.1 (d, $^3J_{FF}$ = 23 Hz, F_o), −168.8 (t, $^3J_{FF}$ = 21 Hz, F_p), −171.0 (t, $^3J_{FF}$ = 20 Hz, F_m). ^{11}B NMR (d_8-THF, 128.8 MHz, 296 K): δ (ppm) −14.6 (br).

[(Bn$_2$Cyclam)Zr(Me)][MeB(C$_6$F$_5$)$_3$] (10). Method A: At room temperature, a J-Young NMR tube was charged with complex **2** (20 mg, 0.04 mmol) and B(C_6F_5)$_3$ (21 mg, 0.04 mmol), and approximately 0.5 mL of CD_2Cl_2 was added to the mixture. The formation of a yellow solution was immediately observed. ^{1}H NMR (CD_2Cl_2, 300.1 MHz, 296 K): δ (ppm) 7.43−7.26 (overlapping, 10H, *H*-Ph), 4.00−3.93 (overlapping, 6H total, 2H, PhCH_2N, 2H, [C3]CH_2N and 2H, [C2]CH_2N), 3.77 (d, 2H, $^2J_{HH}$ = 12 Hz, PhCH_2N), 3.51−3.36 (overlapping, 6H total, 2H, [C3]CH_2N and 4H, [C2]CH_2N), 3.12−3.00 (overlapping, 4H total, 2H, [C3]CH_2N and 2H, [C2]CH_2N), 2.88 (m, 2H, [C3]CH_2N), 2.17 (m, 2H, $CH_2CH_2CH_2$), 2.00 (m, 2H, $CH_2CH_2CH_2$), 0.49 (s, 3H, BCH_3). ^{13}C{^{1}H} NMR (CD_2Cl_2, 75.5 MHz, 296 K): δ (ppm) 150.4 (br, C_6F_5), 147.2 (br, C_6F_5), 139.6 (br, C_6F_5), 138.6 (br, C_6F_5), 136.4 (br, C_6F_5), 135.3 (br, C_6F_5), 132.1 (*o*-Ph or *m*-Ph), 131.1 (*p*-Ph), 130.5 (*o*-Ph or *m*-Ph), 127.7 (*i*-Ph), 58.5 ([C3]CH$_2$N), 56.2 (PhCH$_2$N), 52.8 (overlapping, 2C, [C3]CH$_2$N and [C2]CH$_2$N), 52.2 ([C2]CH$_2$N), 24.8 ($CH_2CH_2CH_2$), 11.0 (br, BCH$_3$). ^{19}F{^{1}H} NMR (CD_2Cl_2, 282.4 MHz, 296 K): δ (ppm) −133.1 (d, $^3J_{FF}$ = 20 Hz, F_o), −165.0 (t, $^3J_{FF}$ = 20 Hz, F_p), −167.7 (dt, $^3J_{FF}$ = 20 Hz, $^4J_{FF}$ = 7 Hz, F_m). ^{11}B{^{1}H} NMR (CD_2Cl_2, 96.3 MHz, 296 K): δ (ppm) −14.9 (s). MS (ESI): *m*/*z* 526.9 [MeB(C_6F_5)$_3$]$^-$.

Method B: A solution of **2** (21 mg, 0.04 mmol) in CD_2Cl_2 was transferred to a J-Young NMR tube and frozen in a liquid nitrogen bath. A solution of B(C_6F_5)$_3$ (22 mg, 0.04 mmol) was added, and the NMR tube was sealed. The tube was then placed in an ethanol/liquid nitrogen bath at −80 °C and yielded a yellow solution. The tube was rapidly transferred into the NMR spectrometer (precooled to −80 °C), and NMR data were recorded from −80 to 25 °C. The spectra show a mixture of species **10** and **11**. NMR data for **11**: ^{19}F{^{1}H} NMR (CD_2Cl_2, 282.4 MHz, 296 K): δ (ppm) −136.3 (d, $^3J_{FF}$ = 23 Hz, F_o), −162.0 (t, $^3J_{FF}$ = 20 Hz, F_p), −165.7 (t, $^3J_{FF}$ = 19 Hz, F_m). ^{11}B NMR (CD_2Cl_2, 96.3 MHz, 296 K): δ (ppm) −4.2 (br).

[(Bn$_2$Cyclam)Zr(Me)(THF)][MeB(C$_6$F$_5$)$_3$] (12). A vial was charged with **2** (0.03 g, 0.06 mmol) and dissolved in 0.5 mL of d_8-THF. A solution of B(C_6F_5)$_3$ (0.3 g, 0.06 mmol) was added dropwise, and the NMR spectra were recorded after 1 h, showing only signals attributed to complex **12**. ^{1}H NMR (d_8-THF, 400.1 MHz, 296 K): δ (ppm) 7.40 (br, 10H total, *H*-Ph), 4.52 (d, 2H, $^2J_{HH}$ = 14 Hz, PhCH_2N), 4.27 (br, 2H, PhCH_2N), 3.80 (overlapping, 4H total, [C2]NCH_2), 3.24 (m, 2H, [C3]NCH_2), 3.19 (m, 2H, [C2]NCH_2), 3.09 (m, 2H, [C3]NCH_2), 2.90 (m, 2H, [C2]NCH_2), 2.75 (m, 2H, [C3]NCH_2), 2.60 (m, 2H, [C3]NCH_2), 1.96 (m, 2H, $CH_2CH_2CH_2$), 1.59 (m, 2H, $CH_2CH_2CH_2$), 0.51 (br, 3H, CH_3B), 0.23 (s, 3H, ZrCH_3). ^{13}C{^{1}H} NMR (d_8-THF, 100.6 MHz, 296 K): δ (ppm) 149.6 (br, C_6F_5), 147.2 (br, C_6F_5), 138.7 (br, C_6F_5), 137.6 (br, C_6F_5), 136.3 (br, C_6F_5), 135.2 (br, C_6F_5), 132.9 (*Ph*CH$_2$N), 128.8 (*Ph*CH$_2$N), 128.1 (*i*-PhCH$_2$N), 56.8 (PhCH$_2$N), 56.1 ([C3]NCH$_2$), 52.8 (overlapping, [C2]NCH$_2$), 50.5 ([C3]NCH$_2$), 41.3 (ZrCH$_3$), 24.9 (CH$_2$CH$_2$CH$_2$), 10.2 (br, BCH$_3$). ^{19}F NMR (d_8-THF, MHz, 296 K): δ (ppm) −135.0 (d, $^3J_{FF}$ = 23 Hz, F_o), −169.1 (t, $^3J_{FF}$ = 21 Hz, F_p), −171.2 (t, $^3J_{FF}$ = 20 Hz, F_m). ^{11}B NMR (d_8-THF, 128.8 MHz, 296 K): δ (ppm) −16.8 (br).

Reaction of [(Bn$_2$Cyclam)Zr(Me)$_2$] (2) with B(C$_6$F$_5$)$_3$ in Toluene-d_8. A solution of **2** (19 mg, 0.04 mmol) in toluene-d_8 was transferred to a J-Young NMR tube and frozen in a liquid nitrogen bath. A solution of B(C_6F_5)$_3$ (19 mg, 0.04 mmol) was

added, and the NMR tube was sealed. The tube was then placed in an ethanol/liquid nitrogen bath at −80 °C and yielded a pale yellow solution, and an orange oil settled on the bottom of the tube. The tube was rapidly transferred into the NMR spectrometer (precooled to −80 °C), and NMR data were recorded from −80 to 25 °C.

[(Bn$_2$Cyclam)Zr(Me)(Tol)][MeB(C$_6$F$_5$)$_3$] (13). ^{1}H NMR (d_8-toluene, 500.1 MHz, 296 K): δ (ppm) 6.88 (m, 4H, *m*-PhCH$_2$N), 6.71 (m, 4H, *o*-PhCH$_2$N), overlapping with C$_7$D$_8$ (*p*-PhCH$_2$N), 3.51−3.45 (overlapping with **14**, 2H, [C3]C*H*$_2$N), 3.32 (d, 2H, $^2J_{HH}$ = 14 Hz, PhC*H*$_2$N), 3.24 (m, 2H, [C2]C*H*$_2$N), 3.17 (d, 2H, $^2J_{HH}$ = 14 Hz, PhC*H*$_2$N), 2.86−2.76 (overlapping with **14**, 4H, [C2]C*H*$_2$N), 2.54 (m, 2H, [C3]C*H*$_2$N), 2.41−2.34 (overlapping with **14**, 2H, [C3]C*H*$_2$N), 2.31 (m, 2H, [C2]C*H*$_2$N), 2.21 (m, 2H, [C3]C*H*$_2$N), 1.50−1.39 (overlapping with **14**, 2H, CH$_2$C*H*$_2$CH$_2$), 1.22−1.16 (overlapping, 5H total, 3H, BC*H*$_3$ and 2H, CH$_2$C*H*$_2$CH$_2$). ^{13}C{^{1}H} NMR (d_8-toluene, 125.8 MHz, 296 K): δ (ppm) 131.3 (*o*-Ph), 130.0 (*m*-Ph), 58.6 ([C3]*C*H$_2$N), 57.3 (Ph*C*H$_2$N), 51.5 ([C2]*C*H$_2$N), 51.1 ([C2]*C*H$_2$N), 50.2 ([C3]*C*H$_2$N), 23.9 (CH$_2$-*C*H$_2$CH$_2$), 11.0 (br, B*C*H$_3$). ^{19}F{^{1}H} NMR (d_8-toluene, 282.4 MHz, 296 K): δ (ppm) −131.8 (dd, br, $^3J_{FF}$ = 18 Hz, F_o), −164.2 (t, $^3J_{FF}$ = 21 Hz, F_p), −166.8 (dt, $^3J_{FF}$ = 24 Hz; $^4J_{FF}$ = 6 Hz, F_m). ^{11}B{^{1}H} NMR (d_8-toluene, 32.2 MHz, 296 K): δ (ppm) −14.4 (br).

(Bn$_2$Cyclam)Zr(C$_6$F$_5$)(CH$_2$B(C$_6$F$_5$)$_2$) (14). ^{1}H NMR (d_8-toluene, 500.1 MHz, 296 K): δ (ppm) 7.06 (m, 4H, *m*-PhCH$_2$N), 6.92 (m, 4H, *o*-PhCH$_2$N), overlapping with C$_7$D$_8$ (*p*-PhCH$_2$N), 5.80 (vb, 2H, BC*H*$_2$), 4.14 (d, 2H, $^2J_{HH}$ = 14 Hz, PhC*H*$_2$N), 3.89 (d, 2H, $^2J_{HH}$ = 14 Hz, PhC*H*$_2$N), 3.51−3.45 (overlapping with **13**, 2H, [C3]C*H*$_2$N), 3.39 (m, 2H, [C2]C*H*$_2$N), 2.86−2.76 (overlapping with **13**, 2H, [C3]C*H*$_2$N), 2.61 (m, 2H, [C2]C*H*$_2$N), 2.49 (m, 2H, [C2]C*H*$_2$N), 2.41−2.34 (overlapping with **13**, 4H total, 2H, [C3]C*H*$_2$N and 2H, [C2]C*H*$_2$N), 1.85 (m, 2H, [C3]C*H*$_2$N), 1.50−1.39 (overlapping with **13**, 2H, CH$_2$C*H*$_2$CH$_2$), 1.33 (m, 2H, CH$_2$C*H*$_2$CH$_2$). ^{13}C{^{1}H} NMR (d_8-toluene, 125.8 MHz, 296 K): δ (ppm) 132.3 (*o*-Ph), overlapping with C$_7$D$_8$ (*m*-Ph), 100.5 (B*C*H$_2$), 55.7 ([C3]*C*H$_2$N), 53.7 ([C3]*C*H$_2$N), 53.3 (Ph*C*H$_2$N), 52.1 ([C2]*C*H$_2$N), 52.0 ([C2]*C*H$_2$N), 25.1 (CH$_2$*C*H$_2$CH$_2$). ^{19}F{^{1}H} NMR (d_8-toluene, 282.4 MHz, 296 K): δ (ppm) −119.0 (m, F_o-Zr(C$_6$F$_5$)), −135.6 (m, F_o-B(C$_6$F$_5$)$_2$), −150.4 (m, F_p-Zr(C$_6$F$_5$)), −158.9 (m, F_m-Zr(C$_6$F$_5$)), −160.6 (t, $^3J_{FF}$ = 21 Hz, F_p-B(C$_6$F$_5$)$_2$), −164.7 (dt, $^3J_{FF}$ = 20 Hz, $^4J_{FF}$ = 7 Hz, F_m-B(C$_6$F$_5$)$_2$). ^{11}B{^{1}H} NMR (d_8-toluene, 32.2 MHz, 296 K): δ (ppm) 86.6 (br).

X-ray Diffraction Experimental Determination. Crystallographic and experimental details of data collection and crystal structure determinations for the two compounds are available in the Supporting Information. Suitable crystals of compounds **3** and **4** were selected and coated in Fomblin oil or an acceptable substitute under an inert atmosphere. Crystals were then mounted on a glass fiber or on a loop external to the glovebox environment. Compounds **3** and **4** were measured on Bruker X8 APEX and Bruker AXS-KAPPA APEX II diffractometers, respectively, both using graphite-monochromated Mo Kα radiation. Data for compounds **3** and **4** were collected at 173(2) and 150(2) K, respectively. Cell parameters were retrieved using Bruker SMART software and refined using Bruker SAINT on all observed reflections.[28]

Absorption corrections were applied using SADABS.[29] The structures were solved by direct methods using SIR92, SIR97, or SIR2004. Structure refinement was done using SHELXL-97. These programs are part of the WinGX software package version 1.70.01.[30]

All non-hydrogen atoms were refined anisotropically. All hydrogen atoms were included in fixed positions. Torsion angles, mean square planes, and other geometrical parameters were calculated using SHELX,[31] just like other experimental details that are given in the Supporting Information. Illustrations of the molecular structures were made with ORTEP3.[32]

In compound **3**, one molecule of cocrystallized toluene was found in the asymmetric unit. As for **4**, one molecule of cocrystallized diethyl ether per two molecules of the compound was found in the asymmetric unit. The diethyl ether fragment was modeled satisfactorily but is highly disordered, resulting in large ellipsoids.

Computational Details. The calculations were performed using the Gaussian 03 software package[33] and the B3LYP functional, without symmetry constraints. That functional includes a mixture of Hartree−Fock[34] exchange with DFT[35] exchange−correlation, given by Becke's three-parameter functional[36] with the Lee, Yang, and Parr correlation functional, which includes both local and nonlocal terms.[22,37] The optimized geometries were obtained with a VDZP basis set (basis b1) consisting of the LanL2DZ basis set[38] augmented with a f-polarization function,[39] for Zr, and a standard 6-31G(d,p)[40] for the remaining elements. Transition-state optimizations were performed with the synchronous transit-guided quasi-Newton method developed by Schlegel et al.[41] Frequency calculations were performed to confirm the nature of the stationary points, yielding one imaginary frequency for the transition states and none for the minima. Each transition state was further confirmed by following its vibrational mode downhill on both sides and obtaining the minima presented on the profiles. Free energy values *in vacuo* were obtained at 298.15 K and 1 atm by conversion of the zero-point-corrected electronic energies with the thermal energy corrections based on the calculated structural and vibrational frequency data. A natural population analysis (NPA)[42] and the resulting Wiberg indices[25] were used to study the electronic structure and bonding of the optimized species. The free energy values presented in the profiles and discussed in the text result from single-point energy calculations using a VTZP basis set (basis b2)

(28) *SAINT*, Version 7.03A; Bruker AXS Inc.: Madison, WI, 1997−2003.
(29) *SADABS*, Bruker Nonius area detector scaling and absorption correction, V2.10; Bruker AXS Inc.: Madison, WI, 2003.
(30) Farrugia, L. J. *J. Appl. Crystallogr.* **1999**, *32*, 837–838.
(31) Sheldrick, G. M. *Acta Crystallogr., Sect. A Found. Crystallogr.* **2008**, *A64*, 112–122.
(32) Farrugia, L. J. *J. Appl. Crystallogr.* **1997**, *30*, 565.
(33) Frisch, M. J. T.; G., W.; Schlegel, H. B.; Scuseria, G. E.; Robb, M. A.; Cheeseman, J. R.; Montgomery, J. A., Jr.; Vreven, T.; Kudin, K. N.; Burant, J. C.; Millam, J. M.; Iyengar, S. S.; Tomasi, J.; Barone, V.; Mennucci, B.; Cossi, M.; Scalmani, G.; Rega, N.; Petersson, G. A.; Nakatsuji, H.; Hada, M.; Ehara, M.; Toyota, K.; Fukuda, R.; Hasegawa, J.; Ishida, M.; Nakajima, T.; Honda, Y.; Kitao, O.; Nakai, H.; Klene, M.; Li, X.; Knox, J. E.; Hratchian, H. P.; Cross, J. B.; Adamo, C.; Jaramillo, J.; Gomperts, R.; Stratmann, R. E.; Yazyev, O.; Austin, A. J.; Cammi, R.; Pomelli, C.; Ochterski, J. W.; Ayala, P. Y.; Morokuma, K.; Voth, G. A.; Salvador, P.; Dannenberg, J. J.; Zakrzewski, V. G.; Dapprich, S.; Daniels, A. D.; Strain, M. C.; Farkas, O.; Malick, D. K.; Rabuck, A. D.; Raghavachari, K.; Foresman, J. B.; Ortiz, J. V.; Cui, Q.; Baboul, A. G.; Clifford, S.; Cioslowski, J.; Stefanov, B. B.; Liu, G.; Liashenko, A.; Piskorz, P.; Komaromi, I.; Martin, R. L.; Fox, D. J.; Keith, T.; Al-Laham, M. A.; Peng, C. Y.; Nanayakkara, A.; Challacombe, M.; Gill, P. M. W.; Johnson, B.; Chen, W.; Wong, M. W.; Gonzalez, C.; Pople, J. A. *Gaussian 03*, Revision C.02; Gaussian, Inc.: Wallingford, CT, 2004.
(34) Hehre, W. J.; Radom, L.; Schleyer, P. v. R.; Pople, J. A. *Ab Initio Molecular Orbital Theory*; John Wiley & Sons: New York, 1986.
(35) Parr, R. G.; Yang, W. *Density Functional Theory of Atoms and Molecules*; Oxford University Press: New York, 1989.
(36) Becke, A. D. *J. Chem. Phys.* **1993**, *98*, 5648–5652.
(37) Lee, C.; Yang, W.; Parr, R. G. *Phys. Rev. B: Condens. Matter* **1988**, *37*, 785–789.
(38) (a) Dunning, T. H., Jr.; Hay, P. J. *Modern Theoretical Chemistry*; Schaefer, H. F., III, Ed.; Plenum: New York, 1976; Vol. *3*, p 1. (b) Hay, P. J.; Wadt, W. R. *J. Chem. Phys.* **1985**, *82*, 270–283. (c) Wadt, W. R.; Hay, P. J. *J. Chem. Phys.* **1985**, *82*, 284–298. (d) Hay, P. J.; Wadt, W. R. *J. Chem. Phys.* **1985**, *82*, 299–310.
(39) Ehlers, A. W.; Boehme, M.; Dapprich, S.; Gobbi, A.; Hoellwarth, A.; Jonas, V.; Koehler, K. F.; Stegmann, R.; Veldkamp, A.; et al. *Chem. Phys. Lett.* **1993**, *208*, 111–114.
(40) (a) Hehre, W. J.; Ditchfield, R.; Pople, J. A. *J. Chem. Phys.* **1972**, *56*, 2257–2261. (b) Hariharan, P. C.; Pople, J. A. *Theor. Chim. Acta* **1973**, *28*, 213–222. (c) Hariharan, P. C.; Pople, J. A. *Mol. Phys.* **1974**, *27*, 209–214. (d) Gordon, M. S. *Chem. Phys. Lett.* **1980**, *76*, 163–168.
(41) (a) Peng, C.; Schlegel, H. B. *Isr. J. Chem.* **1994**, *33*, 449–454. (b) Peng, C.; Ayala, P.; Schlegel, H. B.; Frisch, M. J. *J. Comput. Chem.* **1996**, *17*, 49–56.

with the geometries optimized at the B3LYP/b1 level. Basis b2 consisted of a standard 3-21G[43] with an added f-polarization function[39] for Zr and standard 6-311+G(d,p)[44] for the remaining elements. Solvent (toluene) effects were considered in the PBE1PBE/b2//PBE1PBE/b1 energy calculations using the polarizable continuum model initially devised by Tomasi and co-workers[45] as implemented in Gaussian 03.[46] The molecular cavity was based on the united atom topological model applied on UAHF radii, optimized for the HF/6-31G(d) level.

Acknowledgment. We are grateful to Fundação para a Ciência e Tecnologia, Portugal, and NSERC for funding. We would like to thank Dr. Brian O. Patrick from University of British Columbia for collecting the data of compound **3**. We would also like to thank the Portuguese NMR Network (IST-UTL Centre) for providing access to the NMR.

Supporting Information Available: Table of crystallographic data for **3** and **4**, X-ray crystallographic data for **3** and **4** in CIF format, and coordinates of all computationally optimized structures in PDF format. This material is available free of charge via the Internet at http://pubs.acs.org.

(42) (a) Carpenter, J. E.; Weinhold, F. *J. Mol. Struct.* (*THEOCHEM*) **1988**, *169*, 41–62. (b) Carpenter, J. E. Ph.D. Thesis, University of Wisconsin, Madison, WI, 1987. (c) Foster, J. P.; Weinhold, F. *J. Am. Chem. Soc.* **1980**, *102*, 7211–7218. (d) Reed, A. E.; Weinhold, F. *J. Chem. Phys.* **1983**, *78*, 4066–4073. (e) Reed, A. E.; Weinhold, F. *J. Chem. Phys.* **1985**, *83*, 1736–1740. (f) Reed, A. E.; Weinstock, R. B.; Weinhold, F. *J. Chem. Phys.* **1985**, *83*, 735–746. (g) Reed, A. E.; Curtiss, L. A.; Weinhold, F. *Chem. Rev.* **1988**, *88*, 899–926. (h) Weinhold, F.; Carpenter, J. E. *The Structure of Small Molecules and Ions*; Plenum: New York, 1988; p 227.

(43) (a) Binkley, J. S.; Pople, J. A.; Hehre, W. J. *J. Am. Chem. Soc.* **1980**, *102*, 939–947. (b) Dobbs, K. D.; Hehre, W. J. *J. Comput. Chem.* **1986**, *7*, 359–378. (c) Dobbs, K. D.; Hehre, W. J. *J. Comput. Chem.* **1987**, *8*, 880–893. (d) Dobbs, K. D.; Hehre, W. J. *J. Comput. Chem.* **1987**, *8*, 861–879. (e) Gordon, M. S.; Binkley, J. S.; Pople, J. A.; Pietro, W. J.; Hehre, W. J. *J. Am. Chem. Soc.* **1982**, *104*, 2797–2803. (f) Pietro, W. J.; Francl, M. M.; Hehre, W. J.; DeFrees, D. J.; Pople, J. A.; Binkley, J. S. *J. Am. Chem. Soc.* **1982**, *104*, 5039–5048.

(44) (a) Hay, P. J. *J. Chem. Phys.* **1977**, *66*, 4377–4384. (b) Krishnan, R.; Binkley, J. S.; Seeger, R.; Pople, J. A. *J. Chem. Phys.* **1980**, *72*, 650–654. (c) McGrath, M. P.; Radom, L. *J. Chem. Phys.* **1991**, *94*, 511–516. (d) McLean, A. D.; Chandler, G. S. *J. Chem. Phys.* **1980**, *72*, 5639–5648. (e) Wachters, A. J. H. *J. Chem. Phys.* **1970**, *52*, 1033–1036.

(45) (a) Cances, E.; Mennucci, B.; Tomasi, J. *J. Chem. Phys.* **1997**, *107*, 3032–3041. (b) Cossi, M.; Barone, V.; Mennucci, B.; Tomasi, J. *Chem. Phys. Lett.* **1998**, *286*, 253–260. (c) Mennucci, B.; Tomasi, J. *J. Chem. Phys.* **1997**, *106*, 5151–5158.

(46) (a) Tomasi, J.; Mennucci, B.; Cammi, R. *Chem. Rev.* **2005**, *105*, 2999–3093. (b) Cossi, M.; Scalmani, G.; Rega, N.; Barone, V. *J. Chem. Phys.* **2002**, *117*, 43–54.